Extracting resonance parameters from experimental data on scattering of charged particles.

by

Paul Vaandrager

Submitted in partial fulfilment of the requirements for the degree

Magister Scientiae

in the Department of Physics
in the Faculty of Natural and Agricultural Sciences
University of Pretoria
Pretoria

May 2014

Abstract

Extracting resonance parameters from experimental data on scattering of charged particles.

by

Paul Vaandrager

Supervisor:	Professor S. A. Rakitianski
Degree:	*Magister Scientiae*
Keywords:	Jost matrix, Coulomb potential scattering, S-Matrix, quantum resonance

A method of extracting resonance parameters from scattering data is outlined for scattering that involves Coulomb interactions. This is done for single-channel scattering, as well as multi-channel scattering. Within the outlined model, a set of experimental data points are fitted using a multi-channel S-matrix. The resonance parameters are located as poles of the S-matrix on an appropriate sheet of the Riemann surface of the energy. The proper analytic structure of the S-matrix is ensured, since it is constructed in terms of explicit analytic functions from which the functions depending on the Sommerfield parameters and channel momenta, responsible for the branching of the Riemann surfaces, are factorised. The fashion in which the S-matrix is thus constructed, allows the location of multi-channel and single channel resonances, their partial widths, as well as to obtain the scattering cross sections, even for channels for which no data is available. Pseudo-data for a single- and two-channel model is generated using appropriate potentials for which the resonance parameters are known exactly. Fitting the data appropriately produces resonance parameters which are then compared with the exact values. The feasibility of the proposed model is thus shown.

Samevatting

Die bepaling van resonansieparameters vanuit eksperimentele verstrooiingsdata van gelaaide deeltjies.

deur

Paul Vaandrager

Studieleier: Professor S. A. Rakitianski

Graad: *Magister Scientiae*

Sleutelwoorde: Jost matriks, Coulomb-potensiaal vertstrooiing, S-Matriks, kwantum resonansie

'n Oorsig van 'n metode om resonansieparameters vanuit Coulomb-vestrooiingsdata te verkry, vir enkel- en multikanaal verstrooiing, word weergegee. Binne die raamwerk van die model, word 'n stel eksperimentele datapunte gepas deur gebruik te maak van 'n multikanaal S-matriks. Die resonansieparameters word bepaal as pole van die S-matriks op 'n toepaslike vel van die Riemann-oppervlakte van die energie. Die S-matriks word saamgestel uit eksplisiete analitiese (meromorfiese) funksies, waar die funksies afhanklik van die Sommerfield parameters en kanaalmomenta, wat verantwoordelik is vir die skeiding van die Riemann-oppervlaktes, uitgefaktoriseer is. Dus word die analitiese struktuur van die S-matrix verseker. Sodoende kan enkel- en multikanaal resonansiewaardes en die gepaardgaande resonansiebreedtes bepaal word, asook verstrooiingsdeursnitte, selfs vir kanale waar geen data beskikbaar is nie. Pseudo-data vir 'n enkel- en tweekanaal model word gegenereer deur gebruik te maak van 'n gepaste potentiaal, waarvan resonansieparameters presies bekend is. Die data word op 'n geskikte manier gepas, en sodoende word resonansieparameters verkry en vergelyk met die presiese waardes. Die metode

se geldigheid is dus aangetoon.

Declaration

I, Paul Vaandrager, declare that this dissertation, which I hereby submit in partial fulfilment of the requirements for the degree *Magister Scientiae* at the University of Pretoria, is entirely my own work and has not previously been submitted by me for a degree at this or any other tertiary institution. Where the work of others has been used, every effort is made to correctly reference the source. Furthermore, I cede copyright of this thesis in favour of the University of Pretoria.

Signature:	.....
	Paul Vaandrager
Student number:	27155375
Date:	20th August 2014

Acknowledgements

I wish to extend my sincere gratitude to the following people for their contribution to this dissertation, without whom it would never have reached fruition:

- Professor S. A. Rakitianski , my supervisor, for his guidance, advise and patience.
- My family and friends, for putting up with my complaining, their encouragement in the form of humour, meals and kind words, and, most importantly, for their faith in my abilities.
- My colleagues and the staff at the Department of Physics at the University of Pretoria, especially the tearoom regulars, for providing a bit of sanity in my day. Also to Louwrens van Schalkwyk, for putting this LaTeX 2ε template together, and for his continued assistance with using LaTeX.

Financial Support

Financial support provided by the National Institute for Theoretical Physics (NITheP)[1], with respect to the costs of the study, is hereby acknowledged and is greatly appreciated.

[1]Disclaimer: Any opinions, findings and conclusions or recommendations in this material are those of the author and therefore NITheP does not accept any liability in regard thereto.

Dedications

I dedicate this work to the memory of Amalia Burger, who bullied me into studying Physics (in a nice way).

"You do not really understand something unless you can explain it to your grandmother."

- Albert Einstein

Contents

Chapter 1

Introduction

Most (if not all) problems in quantum mechanics involve determining the bound, resonance or scattering states of a system. Consider the well-studied example of the quantum harmonic oscillator, where only bound states are present [1]. The construction of creation and annihilation operators easily allows bound state energies to be calculated for the harmonic oscillator potential.

Unfortunately, in scattering experiments, it is not always so easy to determine bound state energies for potentials of a different kind, and resonances prove to be even more problematic. Also, bound, resonance and scattering states are all possible states for physical systems. Furthermore, according to Taylor [2], resonances are:

"Probably the most striking phenomenon in the whole range of scattering experiments."

A mathematically rigorous and efficient method of determining the resonance parameters for a scattering problem involving a general potential would thus prove very useful. Since many scattering problems include charged particles, this method should also take into account potentials with a Coulomb tail.

Such a method has been developed in detail by Rakityansky et al [3–9], and the theory will be dealt with in later chapters. The method allows resonance parameters to be extracted from experimental cross-sections by using the analytic structure of the multi-channel Jost matrices for a Coulombic potential. The purpose of this work is to show the feasibility of said method.

For the benefit of the reader unfamiliar with quantum scattering theory, as well as for the sake of completeness, some of the terminology and principal results of scattering theory are briefly discussed. Of particular interest are the Jost matrices, which are fundamental in the formulation of the theory since the well-known S-matrix can be written in terms of the Jost matrices. Also, bound, scattering and resonance states can be calculated in a unified way by means of the Jost matrices [5], as will be shown.

One of the greatest challenges in calculating the Jost matrices for a system is to ensure that all the dependencies on the channel momenta, k, and Sommerfield parameters, η (related to Coulomb scattering), are factorised in the form of an explicit analytic expressions [3]. Knowledge of the analytic structure of such an expression then,

"...allows the deduction of general properties of the physical system even without solving the dynamical equations" [3].

Furthermore, the analytic structure of a complex, single-valued function implies that said function can be approximated with a finite number of terms of the Taylor series [10], which aids greatly in the parametrization of the scattering data.

The problem with the analyticity arises since the Jost matrices, and so also the S-matrix, are not single valued functions of the energy of the system, E (a pre-requisite for analyticity [10]), but depend on k, the corresponding momentum. For the simplest single-channel case, the energy is related to the momentum

by $k = \pm\sqrt{\frac{2\mu E}{\hbar^2}}$, which is double-valued, indicating square-root branching on a Riemann-surface at the threshold energy, $E = 0$. For multi-channel problems, the dependence becomes even more complicated.

Furthermore, the S-Matrix is analytic everywhere except for isolated poles corresponding to the spectral points: the bound and resonance states, which are on the physical and non-physical sheet of the Riemann surface, respectively [3]. Thus knowledge of the splitting of the Riemann surface is fundamentally important.

By following the procedure of [3], the k- and η dependence of the Jost matrices are factorised, ensuring that the remaining unknown functions of the energy are analytic. This is firstly done for the simple single-channel problem, and is then extended to the multi-channel scenario.

In order to test the method, we used artificially generated "experimental" data for a model where the resonance parameters are known exactly. The scattering data is then parametrized as if the problem was not already solved, and resonances are extracted and compared with the true values. This is firstly done for a single-channel problem, and also for a two-channel problem.

Thus it is shown that correctly factorizing the k- and η dependence in the Jost matrices, accurate results for resonances in scattering problems involving Coulombic tails can be obtained. This method is considerably simpler and more efficient than other methods currently used. The effective range expansion can also easily be obtained, if required, from the proposed method: see [3] for example.

Chapter 2

Background Theory

2.1 Introductory scattering theory

"The most important experimental technique in quantum physics is the scattering experiment", according to Taylor [2]. This sentiment can be readily understood, if we consider that most experimental justification for quantum mechanics is obtained from scattering experiments: Rutherford's discovery of the nucleus from the backscattering of alpha particles off gold foil, for example.

Of course, quantum scattering theory is based on quantum mechanics. We are primarily concerned with scattering of non-relativistic particles, thus the Schrödinger picture is quite suitable for our purposes. This is by no means an over-simplification of reality, since many real scattering problems are non-relativistic in nature.

For the quantum scattering problem, the state vector, $|\Psi_a(t)\rangle$, (which fully describes the system) at a specific time is determined by a full set of conserving quantum numbers, $a = \{\alpha_1, \alpha_2, ..., \alpha_N, \}$. These quantum numbers are the eigenvalues of a set of physical operators that commute with each other, and are linear

as well as Hermitian [1].

The time-evolution of the state vector is governed by the time-dependent Schrödinger equation, for which the general solution, at least for a *conserving Hamiltonian*, which is independent of time, is of the form:

$$|\Psi_a(t)\rangle = e^{-iHt}|\psi_a\rangle \tag{2.1}$$

The Hamiltonian, H, for a particle in a central potential U is given in terms of the free-particle Hamiltonian, H^0, as:

$$H = H^0 + U \tag{2.2}$$

with:

$$H^0 = \frac{\hat{\mathbf{p}}^2}{2m} \tag{2.3}$$

Where m is the mass of the particle, and $\hat{\mathbf{p}}$ is the momentum vector operator given by:

$$\hat{\mathbf{p}} = -i\hbar\nabla \tag{2.4}$$

with the del operator given in Cartesian co-ordinates by:

$$\nabla = \left(\frac{\partial}{\partial x}, \frac{\partial}{\partial y}, \frac{\partial}{\partial z}\right) \tag{2.5}$$

If $\hat{\mathbf{r}}$ is the position vector operator, the following commutator relation holds:

$$[\hat{\mathbf{r}}, \hat{\mathbf{p}}] = (i\hbar, i\hbar, i\hbar) \tag{2.6}$$

We will consider a two-body scattering problem, which reduces to a single-body

problem in a central potential. Given two particles with masses m_1 and m_2 as well as positions $\mathbf{r}_1$ and $\mathbf{r}_2$ (relative to some frame of reference), the two-body Hamiltonian is given by:

$$H = H_1^0 + H_2^0 + U(\mathbf{r}_1 - \mathbf{r}_2) \tag{2.7}$$

The potential governing the interaction in a two-body scattering problem, $U(\mathbf{r}_1 - \mathbf{r}_2)$, depends on the radial distance between the two particles. This suggests that the relative co-ordinate, $\mathbf{r}$, should be defined as follows:

$$\mathbf{r} = \mathbf{r_1} - \mathbf{r_2} \tag{2.8}$$

Also, identical to the classical two-body problem, the centre-of-mass co-ordinate is given by:

$$\mathbf{r}_{\text{CM}} = \frac{m_1\mathbf{r}_1 + m_2\mathbf{r}_2}{m_1 + m_2} \tag{2.9}$$

The following is then suggested from the classical two-body problem for the centre of mass momentum, $\mathbf{p}_{\text{CM}}$ and the relative momentum of the two-body system, $\mathbf{p}$:

$$\mathbf{p}_{\text{CM}} = \mathbf{p}_1 + \mathbf{p}_2 \tag{2.10}$$

$$\mathbf{p} = \frac{m_2\mathbf{p}_1 - m_1\mathbf{p}_2}{m_1 + m_2} \tag{2.11}$$

From the above, as well as the commutator relation (2.6), it can easily be shown

that:

$$\begin{aligned}[\hat{\mathbf{r}},\hat{\mathbf{p}}] &= (i\hbar,i\hbar,i\hbar),\\ [\hat{\mathbf{r}}_{\text{CM}},\hat{\mathbf{p}}_{\text{CM}}] &= (i\hbar,i\hbar,i\hbar),\\ [\hat{\mathbf{r}},\hat{\mathbf{p}}_{\text{CM}}] = [\hat{\mathbf{p}}_{\text{CM}},\hat{\mathbf{r}}] &= 0,\end{aligned} \tag{2.12}$$

Thus the suggested definitions of $\mathbf{p}_{\text{CM}}$ and $\mathbf{p}$ are valid [1]. Substituting (2.10), (2.11) and (2.8) into the two-body Hamiltonian (2.7) and simplifying gives:

$$H = \frac{\hat{\mathbf{p}}^2_{\text{CM}}}{2(m_1+m_2)} + \frac{\hat{\mathbf{p}}^2}{2\mu} + U(\mathbf{r}) \tag{2.13}$$

with the reduced mass μ given by:

$$\mu = \frac{m_1 m_2}{m_1+m_2} \tag{2.14}$$

We then assume that the centre of mass frame of reference is stationary relative to the laboratory frame, and so obtain an expression identical to that of a single particle in a central potential:

$$H = \frac{\mathbf{p}^2}{2\mu} + U(\mathbf{r}) = -\frac{\hbar^2}{2\mu}\Delta + U(\mathbf{r}) \tag{2.15}$$

with the Laplacian in Cartesian co-ordinates by:

$$\Delta = \nabla\cdot\nabla = \frac{\partial^2}{\partial x^2} + \frac{\partial^2}{\partial y^2} + \frac{\partial^2}{\partial z^2} \tag{2.16}$$

In a scattering experiment, at a time well before the collision, the single-body-equivalent wave packet is sufficiently far from the localized potential, and will

behave like a free wave packet, governed by H^0. The true state of the system thus becomes experimentally indistinguishable from this "free" state, which is known as the in-asymptote: $|\psi_{in}\rangle$. Similarly, there exists a free state called the out-asymptote, $|\psi_{out}\rangle$, which is experimentally indistinguishable from the true state at a time well after the collision.

This is only true for a potential which satisfies the following conditions [2], which I call the Scattering Potential Conditions:

1. $U(\mathbf{r})$ fall off quicker than r^{-3} as $r \to \infty$.
2. $U(\mathbf{r})$ is less singular than r^{-2} as $r \to 0$.
3. $U(\mathbf{r})$ is continuous for $0 < r < \infty$, apart from a possible finite number of finite discontinuities.

Take note that a potential with a Coulomb tail, which goes as $\frac{1}{r}$, does not satisfy the first condition. This problem is dealt with in Chapter 3.

In general, the interaction region as well as the interaction time are very small. For example, for nuclear reactions, the region of interaction is in the order of $10^{-15}m$ to $10^{-14}m$. Thus it is impossible to observe the true state in practice. This is why we preoccupy ourselves with the in- and out states, which are, theoretically at least, observable.

Now, the evolution of the in-state into the out-state is governed by the Scattering operator, S:

$$|\psi_{out}\rangle = S|\psi_{in}\rangle \tag{2.17}$$

S then contains all the information of experimental interest about the scattering problem [2]. We have thus effectively done away with the actual orbit, but we still need a theoretically obtainable value that can be directly measured: the cross-

section, which is defined as:

"A measure of the probability that a specified particle will be scattered by a specified nucleus or other entity through an angle greater than or equal to a specified angle, θ. ... The differential scattering cross section is a measure of the probability of scattering through an angle lying between θ and $\theta+d\theta$." [11]

By introducing the on-shell T-Matrix, as Taylor [2] does for example, it can be shown that the differential cross section is related to the S-Matrix. The S-Matrix can also be written in terms of the Jost matrices, introduced by Res Jost in 1947 [12] and thus named after him. The Jost matrices are remarkable mathematical objects that allow resonance, bound and scattering states to be calculated in a unified, rigorous way, as has been mentioned before.

Let us thus define the Jost matrices, firstly for a single channel problem. The S-Matrix and differential cross section are then given in terms of the Jost matrices. Generalising to a multi-channel problem is not difficult and follows thereafter.

Note that the Jost matrices reduce to simple 1×1 matrices for a single-channel problem, as will be shown, and are thus referred to as Jost functions for single-channel scattering. Funnily enough, we always refer to the S-Matrix as the S-Matrix, even though for the single-channel problem, it is also a 1×1 matrix.

2.2 The single channel Jost functions and S-matrix

2.2.1 Definition

In the coordinate representation, a state is described by the complex-valued wave function:

$$\langle \mathbf{r} | \Psi_a(t) \rangle = \Psi_a(\mathbf{r}, t) \tag{2.18}$$

The probability density is then given by:

$$\rho(\mathbf{r}) = |\Psi_a(t)|^2 = |\psi_a|^2 \tag{2.19}$$

Schrödinger's equation in this coordinate system becomes:

$$i\hbar\frac{\partial}{\partial t}\Psi_a(\mathbf{r},t) = H\Psi_a(\mathbf{r},t) \tag{2.20}$$

with:

$$\Psi_a(\mathbf{r},t) = e^{-iEt}\psi_a(\mathbf{r}) \tag{2.21}$$

And the time-independent equation is:

$$H\psi_a(\mathbf{r}) = E\psi_a(\mathbf{r}) \tag{2.22}$$

The Hamiltonian for a two-body system is of course given by equation (2.15). Applying the partial wave decomposition for a central potential, as done by any text on quantum mechanics (I like Griffiths [1]), we obtain the radial Schrödinger Equation:

$$\left[\frac{d^2}{dr^2} + k^2 - \frac{\ell(\ell+1)}{r^2} - V(r)\right] u_a(r) = 0 \tag{2.23}$$

Where the wave-momentum, k, and radial potential, $V(r)$ is given by:

$$k^2 = \frac{2\mu E}{\hbar^2} \tag{2.24}$$

$$V(r) = \frac{2\mu U(r)}{\hbar^2} \tag{2.25}$$

The stationary wave function is given in terms of the radial solution and the spher-

ical harmonics:

$$\psi_a(\mathbf{r}) = \frac{u_a(r)}{r} Y_{\ell m}(\theta, \varphi) \tag{2.26}$$

The spherical harmonics are given in terms of the Legendre polynomials P_m^ℓ:

$$Y_\ell^m(\theta, \varphi) = \varepsilon \sqrt{\frac{(2\ell+1)}{4\pi} \frac{(\ell - |m|)!}{(\ell + |m|)!}} e^{im\phi} P_\ell^m(\cos\theta) \tag{2.27}$$

Where θ and φ are the spherical angles, ℓ is the azimuthal quantum number (related to the angular momentum) and m is the magnetic quantum number (related to the direction of the angular momentum vector). Together with the energy, E, the numbers ℓ and m form part of the set, a, of conserving quantum numbers [1].

Let us now consider the radial equation at the boundaries: $r \in [0, \infty)$. If $r \to 0$, $u_a(0) = 0$, as can be seen from (2.26). This is to ensure that $\psi_a(\mathbf{r})$ is finite (normalizable).

If $r \to \infty$, $U(r) \to 0$. This is, of course, not true for all potentials: in general, a potential must obey the Scattering Potential Conditions (from the previous section), specifically the first.

If $U(r)$ is of such a type, as $r \to \infty$ the radial equation (2.23) becomes:

$$\left[\frac{d^2}{dr^2} + k^2 - \frac{\ell(\ell+1)}{r^2}\right] u_a(r) = 0, \qquad r \to \infty \tag{2.28}$$

Solutions to this equation are the pair of linearly-independent Riccati-Hankel functions: $h_\ell^{(\pm)}(kr)$ or the similarly linearly independent pair, the Riccati-Bessel and Riccati-Neumann functions: $j_\ell(kr)$ and $n_\ell(kr)$. The Riccati-Hankel functions are related to the Riccati-Bessel and Riccati-Neumann functions as follows [13]:

$$j_\ell(kr) = \frac{h_\ell^{(+)}(kr) + h_\ell^{(-)}(kr)}{2} \tag{2.29}$$

$$n_\ell(kr) = \frac{h_\ell^{(+)}(kr) - h_\ell^{(-)}(kr)}{2i} \tag{2.30}$$

The general solution to (2.28) is a linear combination of either pair of solutions. The more logical choices of the pair of independent solutions are the Riccati-Hankel functions, since $h_\ell^{(+)}(kr)$ corresponds with an incoming spherical wave, and $h_\ell^{(-)}(kr)$ with an outgoing spherical wave [2]. Thus at large distances we have the linear combination:

$$u_a(r) \xrightarrow[r\to\infty]{} f_\ell^{(in)}(E)h_\ell^{(-)}(kr) + f_\ell^{(out)}(E)h_\ell^{(+)}(kr) \tag{2.31}$$

The amplitudes, $f_\ell^{(in/out)}$, of these incoming and outgoing waves are called the Jost functions [5], and are energy dependent.

Also useful to note is that the Riccati-Hankel functions reduce to simple exponential functions in the same limit:

$$h_\ell^{(\pm)} \xrightarrow[r\to\infty]{} \mp ie^{\pm i(kr-\ell\pi/2)} \tag{2.32}$$

We now know what the Jost functions *are*. The next step is to see how the Jost functions are related to bound, scattering and resonance states, as shown by [3, 5–9].

2.2.2 Bound and resonance States

Bound states are, as the name suggests, stable states of which the particles cannot leave the source of an attractive field. Such states are proper eigenstates of the Hamiltonian, and the energy eigenvalues are real and negative [1]. When a system is in the bound state, since the particle must be localized near the source of the

attractive field (at $r = 0$), the probability of finding the particle far away from the source of the attractive field is zero. Thus the wave function must also be zero far away: $\Psi_a(\mathbf{r},t) \to 0$, and hence $u_a(r) \to 0$ as $r \to \infty$ from (2.26). Since the total energy for such a state must be negative, the momentum, k, must be purely imaginary, by equation (2.24).

By (2.32) this then implies that $h_\ell^{(+)} \to 0$ and $h_\ell^{(-)} \to \infty$ as $r \to \infty$. By (2.31), $u_a(r)$ will then be singular, unless $f_\ell^{(in)}(E_n) = 0$ for specific values of the energy, E_n. Thus bound states can be determined by finding the zeros, or spectral points E_n, of the Jost function with negative energy. Bound states are thus delightfully simple to calculate, and the concept is easy to understand.

In contrast, resonance is a particularly difficult concept to understand, even though it is deeply embedded in the theoretical description of the physical scattering of quantum particles [6]. According to the Penguin Dictionary of Physics [11], quantum resonances are:

"Extremely short-lived elementary particles that decay by strong interaction in about 10^{-24} seconds. ... Resonances may be regarded as excited states of the more stable particles."

The stable particles referred to are, of course, in the bound state. Our understanding of particle stability and decay thus becomes a study of resonance and bound states. In fact, resonance states are often described as semi-bound or quasi-bound states. This is easy to see if we consider quantum resonance physically: particles may be "bound" for a certain time-interval, and then decay. The longer the time interval, the more "bound" the state is, and it becomes more and more difficult to distinguish between true bound states (which last indefinitely) and resonance states.

For an intuitive feel of what resonances are, we can visualize bound and resonance

states as follows: a particle that moves towards a central force, might have such kinetic energy that its trajectory around the source of the central force is closed: it orbits the source of the central force indefinitely. This would correspond to a bound state. For a resonance state, the particle trajectory is *almost* closed: that is, the particle orbits the source of the central force for a number of revolutions and then goes away.

Of course it is meaningless to think of a trajectory in the quantum regime, thus a resonance is more accurately thought of as a partially localized state that slowly dissipates: for discrete frequencies (corresponding to discrete energies), there exists accumulated energy in small regions of space. This energy leaks out through frequency windows called resonance widths. A more rigorous mathematical description of this idea follows.

To obtain such a description, it is important to firstly realise that resonance states, unlike scattering states, do not "remember" how they are formed [5], in the sense that a specific scattering state has a definite in-asymptote and a resonance state does not. For example, the polonium isotope $^{212}_{84}Po$, that can be viewed as a quasi-bound state of the lead isotope $^{208}_{82}Pb$ and an α-particle, could have been formed in a number of different ways; via a multitude of possible nuclear reactions. Yet the $^{212}_{84}Po$ isotope is unstable and will decay at some point, emitting an α-particle and becoming $^{208}_{82}Pb$. If we consider a sample of $^{212}_{84}Po$, in other words considering an ensemble of such resonance states, the α-particles are emitted randomly in all directions with a uniform distribution, i.e. the decay occurs isotropically.

We can thus conclude that only the outgoing spherical wave exists in (2.31) as $r \to \infty$ and that $f_\ell^{(in)}(E) = 0$ for this to occur, similar to the bound state.

Furthermore, one can model the decay of an ensemble of resonance states by the exponential decay law; the prerequisite being that the rate of decay of states is

proportional to the number of states in the system at a specific time. This gives:

$$N(t) = N_0 e^{-\frac{\Gamma}{\hbar}t} \tag{2.33}$$

Where $N(t)$ is the number of states at time t, N_0 is the number of states initially, and Γ is known as the resonance width, measured in units of energy. Thus the ratio $\frac{\Gamma}{\hbar}$ acts as the familiar decay constant. $N(t)$ must be proportional to the probability density (2.19) of the outgoing wave function (which describes the relative motion of the outgoing particles in a decaying system):

$$\rho(\mathbf{r}) \sim N_0 e^{-\frac{\Gamma}{\hbar}t} \tag{2.34}$$

$$\therefore \Psi_{out} \sim e^{-\frac{\Gamma}{2\hbar}t} \tag{2.35}$$

Now, recall the time dependent wave-function (2.21):

$$\Psi_a(\mathbf{r},t) = e^{-iEt}\psi_a(\mathbf{r})$$

If the energy is real, the time-dependent part would be oscillatory, and if the energy has a positive imaginary part, we would have exponential growth in stead of decay. Thus the energy must have a negative imaginary part to ensure proper attenuation, as in (2.35), and it must thus be of the following form:

$$E_n = E_r - \frac{i}{2}\Gamma \tag{2.36}$$

Resonances thus correspond to spectral points E_n which are complex with negative imaginary part, at which the Jost function is zero. In other words, resonances are complex eigenvalues of the Hamiltonian. Yet how is complex energy possible?

Of course resonance energy has no direct physical meaning, but an expression for the half-life of the decaying ensemble of states can be determined in terms of the decay width. The half-life is defined as the time taken for an ensemble of N_0 states to decay to exactly half this initial number of states. Thus:

$$\frac{N_0}{2} = N_0 e^{-\frac{\Gamma}{\hbar} T_{1/2}}$$

Which then gives:

$$T_{1/2} = \frac{\hbar \ln 2}{\Gamma} \tag{2.37}$$

Clearly the imaginary part of the resonance energy is thus hugely important and very useful. The meaning of the real part of (2.36) is equally important, but a little more subtle. It can be shown that $f_\ell^{(in)}(E)$ is analytic (the complex equivalent of being continuous for all E) [4]. If the energy was then to change from a spectral point energy $E_1 = E_{re} + iE_{im}$ where $f_\ell^{(in)}(E_1) = 0$ to a real energy $E_2 = E_{re}$ where $f_\ell^{(in)}(E_2) = C$ where C is some complex value, $f_\ell^{(in)}$ would smoothly transform from 0 to C.

If the imaginary part of E_1, E_{im} is very small, the change in $f_\ell^{(in)}(E)$, thus C, would also be very small. This implies that the change in $f_\ell^{(out)}(E)$ would also have to be small, otherwise the conservation of current would be violated.

This implies that, as the energy of a system changes, around energies $E = E_r$ there will be significant variation in both $f_\ell^{(in)}(E)$ and $f_\ell^{(out)}(E)$, which results in significant variation in the S-Matrix, since it can be shown that the S matrix is related to the Jost functions as follows [2]:

$$S = \frac{f_\ell^{(out)}(E)}{f_\ell^{(in)}(E)} \tag{2.38}$$

The above equation, (2.38) can be considered as the definition of the S matrix, and is quite consistent with more conventional definitions, as can be seen in any text on scattering theory: see Taylor [2] for example.

Variation in the energy of course then results in observable variation in the scattering cross-section, since the S matrix is related to the experimentally measurable cross-section, as has been indicated and will be shown more explicitly in the next chapter.

When the cross-section is plotted against energy, peaks in the cross section often occur at the values of the real part of the complex resonance energy. The real part of resonance energies are thus mostly easily found for sharp peaks in the cross-section data, but, unfortunately, not all data is as easily read, since peaks can be quite wide. Not all peaks correspond with resonances, either.

Also, the measured cross-section, as will be shown, is the sum of all the partial-wave cross sections, where the effect of all the possible resonances add together [4]. Therefore, individual resonances overlap and sharp peaks in the cross-section are no longer easily seen. Such overlap can even occur with resonances of the same partial wave.

For this reason, employing the Jost functions to determine resonances proves much more efficient. As has been indicated, it will be shown how cross-section data can be parametrized to determine the Jost functions, and thus to calculate the resonances.

Firstly, the relationship between the Jost functions and cross section is shown by considering the scattering states.

2.2.3 Scattering states

A scattering state, as stated before, corresponds with a state that has a definite in- and out-asymptote. In contrast, a resonance state does not have a *definite* in-asymptote. The energy of such a scattering state is real and positive [1], which implies that the momentum, k, must also be real and positive. This, in turn, implies that both incoming and outgoing waves of the asymptotics (2.31) oscillate and are finite. Because the particle-flux is conserving, the absolute values of the amplitudes of the incoming and outgoing waves must then be the same:

$$|f_\ell^{(in)}(E)| = |f_\ell^{(out)}(E)|, \qquad E > 0 \tag{2.39}$$

This fact then allows us to prove equation (2.38), since there is a relationship between the so-called phase shift and the S-matrix, as well as between the phase shift and the absolute values of the Jost functions [2].

The plane wave is the solution to a scattering problem with zero potential (the free particle). This is an extreme scattering scenario, since the in-asymptote and the out-asymptote are identical. The plane wave can be written in terms of the spherical harmonics by using the partial wave decomposition:

$$\psi_{\mathbf{k}}(\mathbf{r}) = (2\pi)^{-3/2} e^{i\mathbf{k}\cdot\mathbf{r}} = \sqrt{\frac{2}{\pi}} \frac{1}{kr} \sum_{\ell m} i^\ell j_\ell(kr) Y^*_{\ell m}(\mathbf{k}) Y_{\ell m}(\mathbf{r}) \tag{2.40}$$

It is important to note that the plane wave is not a physically realisable state in itself, and the normalization is not discrete, but an integral over all space yielding the Dirac delta function $\delta(\mathbf{k}' - \mathbf{k})$ [1].

Now, writing the Riccati-Bessel function in terms of the Riccati-Hankel functions

(2.29) the plane wave (2.40) becomes:

$$\psi_{\mathbf{k}}(\mathbf{r}) = \frac{1}{\sqrt{2\pi}kr}\sum_{\ell m} i^{\ell}\left[h_{\ell}^{(-)}(kr) + h_{\ell}^{(+)}(kr)\right] Y_{\ell m}^{*}(\mathbf{k})Y_{\ell m}(\mathbf{r}) \tag{2.41}$$

One should immediately recognise the middle term as the solution to the radial equation: $u_a(r)$ as $r \to \infty$ with the Jost functions $f_{\ell}^{(in/out)}(E) = 1$.

This leads us to propose that the following is a general solution for a scattering problem (where the potential is non-zero):

$$\psi_{\mathbf{k}}(\mathbf{r}) = \frac{1}{\sqrt{2\pi}kr}\sum_{\ell m} i^{\ell}\frac{u_{\ell}(E,r)}{f_{\ell}^{(in)}(E)} Y_{\ell m}^{*}(\mathbf{k})Y_{\ell m}(\mathbf{r}) \tag{2.42}$$

Where $u_{\ell}(E,r)$ is the solution to the radial Schrödinger equation (2.23), and $1/f_{\ell}^{(in)}(E)$ is introduced to ensure correct normalization, as will be indicated. Speaking of normalization, (2.42) is correctly normalized to the Delta function $\delta(\mathbf{k}' - \mathbf{k})$ if and only if:

$$\int_0^{\infty} u_{\ell}(E',r)u_{\ell}(E,r)dr = \frac{2\pi\hbar^2 k}{\mu}|f_{\ell}^{(in)}(E)|^2\delta(E'-E) \tag{2.43}$$

Now, consider (2.42) in the limit as $r \to \infty$, and substitute the solution to the radial

equation in the same limit, (2.31):

$$\begin{aligned}
\psi_{\mathbf{k}}(\mathbf{r}) \quad \xrightarrow[r\to\infty]{} \quad & \frac{1}{\sqrt{2\pi}kr}\sum_{\ell m} i^{\ell}\left[h_{\ell}^{(-)}(kr)+h_{\ell}^{(+)}(kr)\frac{f_{\ell}^{(out)}(E)}{f_{\ell}^{(in)}(E)}\right]Y_{\ell m}^{*}(\mathbf{k})Y_{\ell m}(\mathbf{r}) \\
= \quad & \frac{1}{\sqrt{2\pi}kr}\sum_{\ell m} i^{\ell}\Bigg[h_{\ell}^{(-)}(kr)+h_{\ell}^{(+)}(kr) \\
& -h_{\ell}^{(+)}(kr)+h_{\ell}^{(+)}(kr)\frac{f_{\ell}^{(out)}(E)}{f_{\ell}^{(in)}(E)}\Bigg]Y_{\ell m}^{*}(\mathbf{k})Y_{\ell m}(\mathbf{r}) \\
= \quad & \frac{1}{\sqrt{2\pi}kr}\sum_{\ell m} i^{\ell}\Bigg[\left[h_{\ell}^{(-)}(kr)+h_{\ell}^{(+)}(kr)\right] \\
& +\left[h_{\ell}^{(+)}(kr)\left(\frac{f_{\ell}^{(out)}(E)}{f_{\ell}^{(in)}(E)}-1\right)\right]\Bigg]Y_{\ell m}^{*}(\mathbf{k})Y_{\ell m}(\mathbf{r})
\end{aligned}$$

Using the plane-wave expression in terms of the spherical harmonics (2.40), as

well as the applicable expressions for the Riccati-Hankel functions, (2.32):

$$\begin{aligned}
\psi_{\mathbf{k}}(\mathbf{r}) \xrightarrow[r\to\infty]{} & (2\pi)^{-3/2} e^{i\mathbf{k}\cdot\mathbf{r}} \\
& + \frac{1}{\sqrt{2\pi}kr} \sum_{\ell m} i^{\ell} \left[-ie^{+i(kr-\ell\pi/2)} \left(\frac{f_{\ell}^{(out)}(E)}{f_{\ell}^{(in)}(E)} - 1 \right) \right] Y_{\ell m}^{*}(\mathbf{k}) Y_{\ell m}(\mathbf{r}) \\
= & (2\pi)^{-3/2} e^{i\mathbf{k}\cdot\mathbf{r}} \\
& + \frac{ie^{ikr}}{\sqrt{2\pi}kr} \sum_{\ell m} (-1) \left(ie^{-i\pi/2} \right)^{\ell} \left(\frac{f_{\ell}^{(out)}(E)}{f_{\ell}^{(in)}(E)} - 1 \right) Y_{\ell m}^{*}(\mathbf{k}) Y_{\ell m}(\mathbf{r}) \\
= & (2\pi)^{-3/2} \left[e^{i\mathbf{k}\cdot\mathbf{r}} \right. \\
& \left. + \frac{e^{ikr}}{r} \sum_{\ell m} \frac{4\pi}{2ik} \left(\frac{f_{\ell}^{(out)}(E) - f_{\ell}^{(in)}(E)}{f_{\ell}^{(in)}(E)} \right) Y_{\ell m}^{*}(\mathbf{k}) Y_{\ell m}(\mathbf{r}) \right]
\end{aligned}$$

Now, we apply the addition theorem of spherical harmonics [14]:

$$\begin{aligned}
\psi_{\mathbf{k}}(\mathbf{r}) \xrightarrow[r\to\infty]{} & (2\pi)^{-3/2} \left[e^{i\mathbf{k}\cdot\mathbf{r}} \right. \\
& \left. + \frac{e^{ikr}}{r} \sum_{\ell} \frac{1}{2ik} \left(\frac{f_{\ell}^{(out)}(E) - f_{\ell}^{(in)}(E)}{f_{\ell}^{(in)}(E)} \right) (2\ell+1) P_{\ell}(\cos\theta) \right] \\
\xrightarrow[r\to\infty]{} & (2\pi)^{-3/2} \left[e^{i\mathbf{k}\cdot\mathbf{r}} + \frac{e^{ikr}}{r} \mathbf{f}_{\mathbf{k}}(\mathbf{r}) \right] \qquad (2.44)
\end{aligned}$$

The first term then represents the incoming plane wave in a scattering problem, and the second term the scattered spherical wave. We define the scattering amplitude as:

$$\mathbf{f}_{\mathbf{k}}(\mathbf{r}) = \sum_{\ell} \mathrm{f}_{\ell}(E)(2\ell+1) P_{\ell}(\cos\theta) \qquad (2.45)$$

with the partial wave scattering amplitude defined as:

$$\mathrm{f}_\ell(E) = \frac{1}{2ik}\left(\frac{f_\ell^{(out)}(E)}{f_\ell^{(in)}(E)} - 1\right) \tag{2.46}$$

Equation (2.44) is the postulated scattering solution in most introductory texts, and it is encouraging to confirm the general structure. From this structure it can easily be shown that the differential cross-section is related to the scattering amplitude in the following way:

$$\frac{d\sigma}{d\Omega} = |\mathbf{f}_\mathbf{k}(\mathbf{r})|^2 \tag{2.47}$$

This is because, as Griffiths [1] explains, the probability that the incident particle, travelling at speed v, passes through the infinitesimal area $d\sigma$ in time dt, is given by:

$$dP = |\psi_{incident}|^2 dV = (2\pi)^{-3}(vdt)d\sigma \tag{2.48}$$

This is equal to the probability that the particle scatters into the corresponding solid angle $d\Omega$:

$$dP = |\psi_{scattered}|^2 dV = (2\pi)^{-3}\frac{|\mathbf{f}_\mathbf{k}(\mathbf{r})|^2}{r^2}(vdt)r^2 d\Omega \tag{2.49}$$

Equating the above two equations results in equation (2.47).

Using (2.45) we can now write:

$$\frac{d\sigma}{d\Omega} = |\mathbf{f}_\mathbf{k}(\mathbf{r})|^2 = \sum_\ell \sum_{\ell'} (2\ell+1)(2\ell'+1)\mathrm{f}_\ell^*(E)\mathrm{f}_{\ell'}(E)P_\ell(\cos\theta)P_{\ell'}(\cos\theta)$$

If we take the integral over all directions, apply the orthogonality of the Legendre polynomials [14], and use the expression for the partial scattering amplitudes

(2.46), the following expression is obtained for the total cross section:

$$\sigma = \sum_{\ell} \frac{\pi}{k^2}(2\ell+1)\left|\frac{f_{\ell}^{(out)}(E)}{f_{\ell}^{(in)}(E)} - 1\right|^2 \tag{2.50}$$

For our purposes, the above equation is much more useful in terms of the Jost functions; but by applying equation (2.38) we obtain the well-known relationship between the *S*-Matrix and the cross-section.

The Jost functions thus enable us to calculate bound, resonance and scattering states in a unified way.

Notice that not much is said about the *normalization* of the Jost functions. This is not due to negligence, but is, in fact, because it is not necessary: we either find the zeros of the Jost function, in which case any constant of normalization clearly falls away, or we take the ratio of the Jost functions to find the *S*-Matrix, in which case the normalization constants cancel.

Let us now extend these results to multi-channel scattering.

2.3 The multi-channel Jost matrices and S-matrix

2.3.1 Multi-channel scattering

If we restrict our consideration to two-body scattering, then an N-channel scattering process can be written symbolically as a chemical or nuclear reaction as

follows [6]:

$$A+B \rightarrow \begin{cases} A+B \\ C+D \\ E+F \\ \ldots \end{cases}$$

We understand the above as a collision of two particles, A and B, which then yields A and B again, or C and D, or any other possible pair of particles with varying probability, and two-body systems in both the initial and final states. Typically, when an ensemble of particles are scattered off another ensemble of particles, all possible resulting particle pairs are present, with varying probability. In fact, the majority of possible resulting pairs have a very small probability of being present. A single-channel is thus an oversimplification of reality, but a useful one. See Taylor [2] for further details.

The Hamiltonian for a two-body problem which is reduced to an effective one-body problem when the motion of its centre of mass is separated, can be written as follows:

$$H = H^0 + \mathscr{U} + h \tag{2.51}$$

Where H^0 is the free-motion part, $\mathscr{U}$ is the interaction operator (interaction potential) and h is the Hamiltonian that describes internal dynamics in the moving body, such as internal states of colliding atoms [15]. This equation is similar to equation (2.2) for the single channel, except that we have the extra term h.

Now, each internal state of the body corresponds with a different channel of the scattering process [15]. There is an infinite number of internal states, and thus an infinite number of channels. The eigenstates of h are thus:

$$h|n\rangle = E_n|n\rangle, \qquad n = 1,2,3,\ldots,\infty \tag{2.52}$$

And h is thus given by [1]:

$$h = \sum_{n=1}^{\infty} |n\rangle E_n \langle n| \tag{2.53}$$

We assume that only N states are important [15], the N states with the greatest probabilities of existing, thus h is approximated by:

$$h \approx \sum_{n=1}^{N} |n\rangle E_n \langle n| \tag{2.54}$$

We now sandwich the total Hamiltonian (2.51) between $\langle n|$ and $|n'\rangle$ and use the above approximation for h:

$$\begin{aligned}
\langle n|H|n'\rangle &= \langle n|H^0|n'\rangle + \langle n|\mathscr{U}|n'\rangle + \langle n|h|n'\rangle \\
\therefore H_{nn'} &= -\delta_{nn'}\frac{\hbar^2}{2\mu_n}\Delta_{\mathbf{r}} + \mathscr{U}_{nn'} + \sum_{n=1}^{N}\langle n||n\rangle E_n \langle n||n'\rangle \\
\therefore H_{nn'} &= -\delta_{nn'}\frac{\hbar^2}{2\mu_n}\Delta_{\mathbf{r}} + \mathscr{U}_{nn'} + E_n\delta_{nn'}
\end{aligned} \tag{2.55}$$

The Hamiltonian thus becomes an $N \times N$ matrix, where μ_n is the reduced mass in the channel n. The eigenvalue equation $H\Psi = E\Psi$ then becomes a set of coupled differential equations for the channel wave functions, ψ_n [15]:

$$\left[\frac{\hbar^2}{2\mu_n}\Delta_{\mathbf{r}} + (E - E_n)\right]\psi_n(E,\mathbf{r}) = \sum_{n'=1}^{N}\mathscr{U}_{nn'}(\mathbf{r})\psi_n(E,\mathbf{r}) \tag{2.56}$$

The interaction-potential governing such a process will be a $N \times N$ matrix $\mathscr{U}_{mn}$, with each matrix entry satisfying the *Scattering Potential Conditions* of Chapter 2.1. The wave function describing such a process at the collision energy E is then

the column matrix:

$$\Psi(E,\mathbf{r}) = \begin{pmatrix} \psi_1(E,\mathbf{r}) \\ \psi_2(E,\mathbf{r}) \\ \vdots \\ \psi_n(E,\mathbf{r}) \end{pmatrix} \tag{2.57}$$

Where $n = 1,2,...$ corresponds to separate channels. The channels are not only characterised by the type of particles ($A+B$, $C+D$, etc.) but also by the complete set of channel quantum numbers $a = \{\alpha_1, \alpha_2, ..., \alpha_N, \}$. This means that states with different threshold energy, spin, or angular momentum simply become new channels [2]. Stated differently:

"Any two states of the system that differ by at least one quantum number are considered as different channels, even if the type of the particles and the threshold energies are the same." [6]

This then implies that each channel has a definite value of the angular momentum, thus the angular dependence for each channel state can be factorized:

$$\psi_n(E,\mathbf{r}) = \frac{u_n(E,r)}{r} Y_{\ell_n m_n}(\theta,\varphi) \tag{2.58}$$

Similar to the single channel case, we now obtain a set of coupled radial equations:

$$\left[\partial_r^2 + k_n^2 - \frac{\ell_n(\ell_n+1)}{r^2}\right] u_n(E,r) = \sum_{n'=1}^{N} V_{nn'}(r) u_{n'}(E,r) \tag{2.59}$$

The coupling is due to the off-diagonal elements of the radial interaction-potential matrix $V_{nn'}$ [6], given in terms of $U_{nn'}$ by [15]:

$$V_{nn'}(r) = \frac{2\mu_n}{\hbar^2} \int Y^*_{\ell_n m_n}(\theta,\varphi) U_{nn'}(\mathbf{r}) Y_{\ell_{n'} m_{n'}}(\theta,\varphi)\, \mathrm{d}\Omega_{\mathbf{r}}. \tag{2.60}$$

The channel momenta, k_n, are defined as:

$$k_n = \sqrt{\frac{2\mu_n}{\hbar^2}(E - E_n)} \tag{2.61}$$

The boundary conditions for equation (2.59) are derived from the requirement that any physical solution must be regular at $r = 0$ [2] and have special behaviour at $r \to \infty$. The special behaviour differs for bound, resonant and scattering states, identical to the single channel problem.

Such a system of N linear second-order differential equations as given in (2.59) has $2N$ linearly independent column solutions [15]. Only half of the solutions are regular at the origin, $r = 0$ [10], and the so-called *Fundamental Matrix of the Regular Solutions* is given by combining these regular solutions:

$$\Phi(E,r) = \begin{pmatrix} \phi_{11}(E,r) & \phi_{12}(E,r) & \cdots & \phi_{1N}(E,r) \\ \phi_{21}(E,r) & \phi_{22}(E,r) & \cdots & \phi_{2N}(E,r) \\ \vdots & \vdots & \ddots & \vdots \\ \phi_{N1}(E,r) & \phi_{N2}(E,r) & \cdots & \phi_{NN}(E,r) \end{pmatrix} \tag{2.62}$$

Any particular regular solution of (2.59) must be a linear combination of the columns of the *Fundamental Matrix of the Regular Solutions* [10]:

$$\begin{pmatrix} u_1 \\ u_2 \\ \vdots \\ u_N \end{pmatrix} = C_1 \begin{pmatrix} \phi_{11} \\ \phi_{21} \\ \vdots \\ \phi_{N1} \end{pmatrix} + C_2 \begin{pmatrix} \phi_{12} \\ \phi_{22} \\ \vdots \\ \phi_{N2} \end{pmatrix} + \cdots + C_N \begin{pmatrix} \phi_{1N} \\ \phi_{2N} \\ \vdots \\ \phi_{NN} \end{pmatrix}$$

Or, more compactly:

$$\begin{pmatrix} u_1 \\ u_2 \\ \vdots \\ u_N \end{pmatrix} = \begin{pmatrix} \phi_{11}(E,r) & \phi_{12}(E,r) & \cdots & \phi_{1N}(E,r) \\ \phi_{21}(E,r) & \phi_{22}(E,r) & \cdots & \phi_{2N}(E,r) \\ \vdots & \vdots & \ddots & \vdots \\ \phi_{N1}(E,r) & \phi_{N2}(E,r) & \cdots & \phi_{NN}(E,r) \end{pmatrix} \begin{pmatrix} C_1 \\ C_2 \\ \vdots \\ C_N \end{pmatrix} \tag{2.63}$$

Correct behaviour when $r \to 0$ is thus guaranteed, and proper choice of the combination coefficients C_N results in correct asymptotic behaviour (when $r \to \infty$).

2.3.2 Jost matrices

As with the single-channel problem, the potential matrix $V_{nn'}$ in equation (2.59) tends to zero when $r \to \infty$, that is, when the scattered particles move far apart. We are still strictly referring to a potential which satisfies the *Scattering Potential Conditions*. Thus we are left with a set of N second-order equations:

$$\left[\partial_r^2 + k_n^2 - \frac{\ell_n(\ell_n+1)}{r^2}\right] u_n(E,r) \approx 0, \qquad r \to \infty \tag{2.64}$$

Which are no longer coupled, since the term responsible for the coupling has disappeared. There are $2N$ linearly independent column solutions (two linearly-independent solutions for each equation), which can be written as two diagonal square matrices involving the Riccati-Hankel functions $h_\ell^{(\pm)}(kr)$ [6]:

$$W^{(in)} = \begin{pmatrix} h_{\ell_1}^{(-)}(k_1 r) & 0 & \cdots & 0 \\ 0 & h_{\ell_2}^{(-)}(k_2 r) & \cdots & 0 \\ \vdots & \vdots & \ddots & \vdots \\ 0 & 0 & \cdots & h_{\ell_N}^{(-)}(k_N r) \end{pmatrix} \tag{2.65}$$

$$W^{(out)} = \begin{pmatrix} h^{(+)}_{\ell_1}(k_1 r) & 0 & \cdots & 0 \\ 0 & h^{(+)}_{\ell_2}(k_2 r) & \cdots & 0 \\ \vdots & \vdots & \ddots & \vdots \\ 0 & 0 & \cdots & h^{(+)}_{\ell_N}(k_N r) \end{pmatrix} \tag{2.66}$$

Any particular column solution to (2.64) can be written as a linear combination of the $2N$ columns of (2.65) and (2.66), since they form a basis in the space of solutions of (2.64) [15].

At $r \to \infty$, the columns of matrix (2.62), the *Fundamental Matrix of the Regular Solutions*, have to be solutions of (2.64). Thus, (2.62) can be written as a linear combination of (2.65) and (2.66), at large r [15]:

$$\Phi(E,r) \xrightarrow[r\to\infty]{} W^{(in)}(E,r) f^{(in)}(E) + W^{(out)}(E,r) f^{(out)}(E) \tag{2.67}$$

$f^{(in/out)}(E)$ are then defined as the Jost matrices, and it is easy to see that for $N = 1$ our derivations and definitions are identical to a 1-channel scenario. The S-matrix is then given by [6, 15, 16]:

$$S(E) = f^{(out)}(E) \left[f^{(in)}(E) \right]^{-1} \tag{2.68}$$

The spectral points $E = \mathscr{E}_n$ that relate to bound and resonance states, are those energy values where the inverse of the matrix $f^{(in)}(E)$ does not exist, that is, where:

$$\det f^{(in)}(E) = 0 \tag{2.69}$$

The channel cross-section is given by [2]:

$$\sigma_{mn}(E) = \frac{\pi}{k_m^2}(2\ell_m + 1)\,|S_{nm}(E) - \delta_{mn}|^2 \tag{2.70}$$

For a two-channel problem, as we will be looking at, $N = 2$. An explicit derivation of the above results for a two-channel problem is given in [16], which gives exactly the same result, but is easier to follow.

This is all very well, but the focus of this work is to obtain meaningful results for Coulomb scattering. In the next chapter we find expressions for the Jost functions for such scattering problems

Chapter 3

Coulomb scattering

3.1 Single channel Jost functions for Coulomb scattering

An effective way to deal with a scattering problem involving Coulomb interactions is difficult. The standard formalism of scattering theory breaks down significantly when such a potential is considered. According to Taylor [2]:

"...none of the principal results of scattering theory do hold for the Coulomb potential."

Yet there are ways to bypass some of the complexities, especially when the problem is approached in terms of the Jost functions, as done by Rakityansky, Sofianos and Elander [3, 5].

The Coulomb potential does not obey the first of the Scattering Potential Conditions, as mentioned before. Any potential with Coulomb tail can be written as follows:

$$V_C(r) = V_S + \frac{2k\eta}{r} \tag{3.1}$$

Where V_S is a potential of short range, which does obey condition 1, and the second term is the purely Coulomb part. The Sommerfield parameter, η, corresponds to the electric force between two particles of charge eZ_1 eZ_2 [3]:

$$\eta = \frac{\mu e^2 Z_1 Z_2}{k\hbar^2} \tag{3.2}$$

Notice that the behaviour of a purely Coulomb system, without short-range part, would differ from the system with both short-range potential and Coulomb tail, since the processes,

"...are modified at small distances by some short-range force", according to Taylor [2]. The radial equation for a potential with Coulomb tail can then be written as follows:

$$\left[\frac{d^2}{dr^2} + k^2 - \frac{\ell(\ell+1)}{r^2} - V_S - \frac{2k\eta}{r}\right] u_a(r) = 0 \tag{3.3}$$

Now as $r \to \infty$, the short range part, V_S, disappears, as before. We then have:

$$\left[\frac{d^2}{dr^2} + k^2 - \frac{\ell(\ell+1)}{r^2} - \frac{2k\eta}{r}\right] u_a(r) = 0, \qquad r \to \infty \tag{3.4}$$

The general solutions to the above is a linear combination of the so-called regular and irregular Coulomb functions, $F_\ell(\eta, kr)$ and $G_\ell(\eta, kr)$ [2, 3, 17]. In essence, the problems that arise due to the Coulombic part of the radial equation are now embedded in these two functions. It is clear, then, that the Regular and Irregular Coulomb functions are significantly more difficult to deal with than the Riccati-Hankel, -Neumann and -Bessel functions; especially computationally. But, we can deal with them, and so it is postulated that the solution to (3.3) must be a linear combination of these two functions at all r-values:

$$u_\ell(E,r) = F_\ell(\eta, kr)A_\ell(E,r) + G_\ell(\eta, kr)B_\ell(E,r) \tag{3.5}$$

If $r \to \infty$, beyond the range of the potential V_S, the functions $A_\ell(E,r)$ and $B_\ell(E,r)$ would become r -independent [3]. Now, by applying the well-known method of variation of parameters [10] the following equivalent system of first-order differential equations is obtained. Note that the symbols (E,r) are omitted to facilitate ease of reading:

$$\partial_r A_\ell = \frac{1}{k} G_\ell V_S (F_\ell A_\ell + G_\ell B_\ell) \tag{3.6}$$

$$\partial_r B_\ell = -\frac{1}{k} F_\ell V_S (F_\ell A_\ell + G_\ell B_\ell) \tag{3.7}$$

Since $u_\ell(E,r)$ is the physical wave function, it must be regular at $r = 0$; that is, it must have a finite derivative at the point $r = 0$ [18]. Also, as the names suggest, the regular Coulomb function is, in fact, regular, and the irregular Coulomb function is not [3, 17]. These facts enable us to make the following, simplest choice of boundary conditions:

$$A_\ell(E,0) = 1\,, \qquad B_\ell(E,0) = 0 \tag{3.8}$$

By this choice of boundary condition, the solution, $u_\ell(E,r)$, must behave like the regular Coulomb function near the origin, which, in turn, can be expressed in terms of the Coulomb barrier factor, $C_\ell(\eta)$, at the same limit:

$$u_\ell(E,r) \xrightarrow[r\to 0]{} F_\ell(\eta,kr) \xrightarrow[r\to 0]{} (kr)^{\ell+1} C_\ell(\eta) \tag{3.9}$$

with the Coulomb barrier factor given by [3, 17]:

$$C_\ell(\eta) = \frac{2^\ell e^{-\pi\eta/2}}{\Gamma(2\ell+2)} \left|\Gamma(\ell+1\pm i\eta)\right| \tag{3.10}$$

Also note the specific behaviour of the regular and irregular Coulomb functions for large r [2]:

$$F_\ell(\eta,kr) \xrightarrow[r\to\infty]{} \sin\left(kr-\eta\ln(2kr)-\frac{\ell\pi}{2}+\sigma_\ell\right) \tag{3.11}$$

$$G_\ell(\eta,kr) \xrightarrow[r\to\infty]{} \cos\left(kr-\eta\ln(2kr)-\frac{\ell\pi}{2}+\sigma_\ell\right) \tag{3.12}$$

Where σ_ℓ is the Coulomb phase shift, given by:

$$\sigma_\ell = \arg\Gamma(\ell+1+i\eta) \tag{3.13}$$

Now, the regular solution, $\phi_\ell(E,r)$, is defined as the solution to the radial equation, (2.23), for any potential, that behaves exactly like the Riccati-Bessel function for very small r [2]:

$$\phi_\ell(E,r) \xrightarrow[r\to 0]{} j_\ell(kr) \xrightarrow[r\to 0]{} \frac{(kr)^{\ell+1}}{(2\ell+1)!!} \tag{3.14}$$

When comparing the regular solution (3.14) to (3.9) at small r, the following should hold for all r:

$$\phi_\ell(E,r) = \frac{1}{C_\ell(\eta)(2\ell+1)!!}u_\ell(E,r) \tag{3.15}$$

Recall that the Jost functions were defined from the asymptotic behaviour of (2.31), which is the regular solution to the non-Coulomb radial equation at large r, (2.28). Thus we want to determine the asymptotic behaviour of the regular solution with Coulomb interaction, since we want to introduce the Jost functions for a

Coulomb potential. The following is proposed:

$$\phi_\ell(E,r) \xrightarrow[r\to\infty]{} h_\ell^{(-)}(kr)e^{+i\eta\ln 2kr} f_\ell^{(in)}(E) + h_\ell^{(+)}(kr)e^{-i\eta\ln 2kr} f_\ell^{(out)}(E) \tag{3.16}$$

Where the usual incoming- and outgoing waves are modified by $e^{\pm i\eta\ln 2kr}$, but the Jost functions are defined as before: the asymptotic behaviour of the energy-dependent amplitudes of the incoming and outgoing spherical waves. The validity of this proposal is shown, but a more rigorous proof is given by Farina [19] and Watson [13]. We begin by writing the radial equation with Coulomb tail, (3.3), as follows:

$$\frac{d^2 z_a(r)}{dr^2} + \left[k^2 - W(r)\right] z_a(r) = 0 \tag{3.17}$$

with $W(r)$ given by:

$$W(r) = \frac{\ell(\ell+1)}{r^2} + V_S + \frac{2k\eta}{r} \tag{3.18}$$

Now, with A being a constant and $g(r)$ an unknown function, we follow the procedure of Farina [19] and let:

$$z_a^{(\pm)}(r) = A\exp\left[\left(\int g(r)dr\right) \pm ikr\right] \tag{3.19}$$

When this is substituted into (3.17) and by applying the fundamental theorem of Calculus [10], the following is obtained:

$$\frac{dg}{dr} + (g(r))^2 \pm 2ikg(r) = W(r) \tag{3.20}$$

In equation (3.18), since V_S is of short-range, and the r^{-2} term dies off quicker than the r^{-1} term, it can be seen that the asymptotic behaviour of $W(r)$ is as

follows:

$$W(r) \xrightarrow[r\to\infty]{} \frac{2k\eta}{r} \tag{3.21}$$

Thus (3.20) for large r becomes:

$$\frac{dg}{dr} + (g(r))^2 \pm 2ikg(r) \sim \frac{2k\eta}{r}, \qquad r \to \infty \tag{3.22}$$

This can only be the case if the asymptotic behaviour of $g(r)$ is as follows:

$$g(r) \xrightarrow[r\to\infty]{} \mp\frac{i\eta}{r} \tag{3.23}$$

Thus the asymptotic behaviour of $z_a^{(\pm)}(r)$ can be found from (3.23) and (3.19):

$$\begin{aligned} z_a^{(\pm)}(r) \quad &\xrightarrow[r\to\infty]{} \quad A\exp\left[\left(\mp\int\frac{i\eta}{r}dr\right)\pm ikr\right] \\ &= \quad Ae^{\mp i\eta\ln cr\pm ikr} \\ &= \quad e^{\pm ikr+C_\ell\mp i\eta\ln cr} \end{aligned} \tag{3.24}$$

Where c and C_ℓ are constants. The final solution would then be a linear combination of the above solutions, and the general form then agrees with our proposed solution, (3.16), if the asymptotic behaviour of the Riccati-Hankel functions are implemented.

Now we proceed as [3] again; in the same way that the Riccati-Hankel functions can be written in terms of the Riccati-Bessel and Riccati-Neumann functions (by using (2.29) and (2.30)):

$$h_\ell^{(\pm)}(kr) = j_\ell(kr) \pm in_\ell(kr)$$

We define the following functions in terms of the regular and irregular Coulomb functions:

$$H_\ell^{(\pm)}(\eta,kr) = F_\ell(\eta,kr) \mp iG_\ell(\eta,kr) \tag{3.25}$$

The asymptotic behaviour of which can be determined with (3.11) and (3.12):

$$\begin{aligned} H_\ell^{(\pm)}(\eta,kr) &\xrightarrow[r\to\infty]{} \sin\left(kr-\eta\ln(2kr)-\frac{\ell\pi}{2}+\sigma_\ell\right) \\ &\quad \mp i\cos\left(kr-\eta\ln(2kr)-\frac{\ell\pi}{2}+\sigma_\ell\right) \\ &= \mp i\left[\cos\left(kr-\eta\ln(2kr)-\frac{\ell\pi}{2}+\sigma_\ell\right)\right. \\ &\quad \left.\pm i\sin\left(kr-\eta\ln(2kr)-\frac{\ell\pi}{2}+\sigma_\ell\right)\right] \\ \therefore H_\ell^{(\pm)}(\eta,kr) &\xrightarrow[r\to\infty]{} \mp i\exp\left[\mp i\left(kr-\eta\ln(2kr)-\frac{\ell\pi}{2}+\sigma_\ell\right)\right] \end{aligned} \tag{3.26}$$

In terms of the above, we can then re-write the regular solution (3.16) as follows:

$$\phi_\ell(E,r) \xrightarrow[r\to\infty]{} H_\ell^{(-)}(\eta,kr)e^{i\sigma}f_\ell^{(in)}(E) + H_\ell^{(+)}(\eta,kr)e^{-i\sigma}f_\ell^{(out)}(E) \tag{3.27}$$

If (3.15), the relation between the regular solution and the actual solution, is then used:

$$\begin{aligned} u_\ell(E,r) &\xrightarrow[r\to\infty]{} H_\ell^{(-)}(\eta,kr)C_\ell(\eta)(2\ell+1)!!\,e^{i\sigma}f_\ell^{(in)}(E) \\ &\quad + H_\ell^{(+)}(\eta,kr)C_\ell(\eta)(2\ell+1)!!\,e^{-i\sigma}f_\ell^{(out)}(E) \end{aligned} \tag{3.28}$$

We now define the following in terms of the unknown functions $A_\ell(E,r)$ and

$B_\ell(E,r)$:

$$\mathscr{F}_\ell^{(in/out)}(E,r) = \frac{1}{2}\left[A_\ell(E,r) \mp iB_\ell(E,r)\right] \tag{3.29}$$

with the following boundary conditions obtained from (3.8):

$$\mathscr{F}_\ell^{(in/out)}(E,0) = \frac{1}{2} \tag{3.30}$$

This then allows us to write:

$$u_\ell(E,r) = H_\ell^{(-)}(\eta,kr)\mathscr{F}_\ell^{(in)}(E,r) + H_\ell^{(+)}(\eta,kr)\mathscr{F}_\ell^{(out)}(E,r) \tag{3.31}$$

This is easily shown to be valid, since (3.5) is obtained if (3.29) and (3.25) is substituted into the above. By taking the limit as $r \to \infty$ and comparing with (3.28) the following is obtained:

$$f_\ell^{(in/out)}(E) = \frac{e^{\mp i\sigma_\ell}}{C_\ell(\eta)(2\ell+1)!!}\lim_{r\to\infty}\mathscr{F}_\ell^{(in/out)}(E,r) \tag{3.32}$$

And finally, we combine (3.32) and (3.29) to obtain:

$$f_\ell^{(in/out)}(E) = \frac{e^{\mp i\sigma_\ell}}{2C_\ell(\eta)(2\ell+1)!!}\left\{A_\ell(E,\infty) \mp iB_\ell(E,\infty)\right\} \tag{3.33}$$

All that remains, then, is to determine the functions $A_\ell(E,r)$ and $B_\ell(E,r)$ from the coupled set of differential equations (3.6) and (3.7), if the potential is known. If not, as in our case, scattering data can be fitted to the power series expansions of $A_\ell(E,r)$ and $B_\ell(E,r)$, allowing the determination of the fitting parameters of the expansion, which in turn allows the calculation of $A_\ell(E,r)$ and $B_\ell(E,r)$. Either way, the Jost functions can then be calculated with (3.33). The scattering problem is then solved, since all important information can be gained from the Jost

functions, as has been shown in Chapter 2.

Unfortunately, fitting the power-series expansion of $A_\ell(E,r)$ and $B_\ell(E,r)$ to the data is not so simple. This is because a complex-valued function can only be written as a power-series expansion if it is an entire function, [10], which is not necessarily the case with $A_\ell(E,r)$ and $B_\ell(E,r)$. Furthermore, the wave-momentum k is embedded in both functions, and since it is the square of the energy, E, that is related to k by equation (2.24), a splitting of the Riemann surface into the so-called physical and non-physical sheet occurs. Therefore, we first need to isolate the k-dependence of the two functions to ensure analyticity, as indicated in the Introduction. This will be done in the next chapter.

One may also wonder why we solve the set of differential equations involving $A_\ell(E,r)$ and $B_\ell(E,r)$, and not solve for the Jost functions directly. This is due to computational instability of the Jost functions at large r, the Jost functions being exponential in nature. Conversely, the functions $A_\ell(E,r)$ and $B_\ell(E,r)$ are sinusoidal for most values of r, and exponentially growing for very small r. So, in fact, for reliable results and stable code, one effectively makes use of both sets of differential equations, depending on the regime of r.

3.2 Analytic structure of single-channel Jost functions

Let us now deal with the troublesome k- and η-dependence of $A_\ell(E,r)$ and $B_\ell(E,r)$. This is done by firstly using the results of Lambert [20], who derives the structure of the Regular and Irregular Coulomb functions in terms of the entire

(analytic and single-valued) functions, $\tilde{F}_\ell(E,r)$ and $\tilde{G}_\ell(E,r)$, as follows:

$$F_\ell(\eta,kr) = D_\ell(\eta,k)\tilde{F}_\ell(E,r) \tag{3.34}$$

$$G_\ell(\eta,kr)) = M(\eta)D_\ell(\eta,k)\tilde{F}_\ell(E,r) + \frac{k}{D_\ell(\eta,k)}\tilde{G}_\ell(E,r) \tag{3.35}$$

Where the k- and η-dependence is explicitly isolated via the expressions:

$$D_\ell(\eta,k) = C_\ell(\eta)k^{\ell+1}, \qquad M(\eta) = \frac{2\eta h(\eta)}{C_0^2(\eta)} \tag{3.36}$$

with:

$$h(\eta) = \frac{1}{2}\left[\psi(i\eta)+\psi(-i\eta)\right] - \ln\hat{\eta}, \qquad \psi(z) = \frac{\Gamma'(z)}{\Gamma(z)}, \qquad \hat{\eta} = \frac{\mu e^2|Z_1Z_2|}{k\hbar^2} \tag{3.37}$$

If (3.34) is then substituted into the radial wave function (3.5), the following is obtained:

$$u_\ell(E,r) = D_\ell(\eta,k)\Big[\left(A_\ell(E,r)+M(\eta)B_\ell(E,r)\right)\tilde{F}_\ell(E,r) + \frac{k}{D_\ell^2(\eta,k)}B_\ell(E,r)\tilde{G}_\ell(E,r)\Big] \tag{3.38}$$

We then define the following two functions:

$$\tilde{A}_\ell(E,r) = A_\ell(E,r)+M(\eta)B_\ell(E,r) \tag{3.39}$$

$$\tilde{B}_\ell(E,r) = \frac{k}{D_\ell^2(\eta,k)}B_\ell(E,r) \tag{3.40}$$

Rakityansky [3] then shows that the following can be obtained from the above definition, from equation (3.38) and from the system of differential equations (3.6)

and (3.7):

$$\partial_r \tilde{A}_\ell(E,r) = \tilde{G}_\ell(E,r)V(r)\left[\tilde{F}_\ell(E,r)\tilde{A}_\ell(E,r)+\tilde{G}_\ell(E,r)\tilde{B}_\ell(E,r)\right] \quad (3.41)$$

$$\partial_r \tilde{B}_\ell(E,r) = -\tilde{F}_\ell(E,r)V(r)\left[\tilde{F}_\ell(E,r)\tilde{A}_\ell(E,r)+\tilde{G}_\ell(E,r)\tilde{B}_\ell(E,r)\right] \quad (3.42)$$

From (3.8) it can also be shown that:

$$\tilde{A}_\ell(E,0) = 1\,, \qquad \tilde{B}_\ell(E,0) = 0 \quad (3.43)$$

Thus, since $\tilde{F}_\ell(E,r)$ and $\tilde{G}_\ell(E,r)$ are entire functions, it follows from the Poincaré theorem that $\tilde{A}_\ell(E,r)$ and $\tilde{B}_\ell(E,r)$ are also entire functions of E for any finite r [3]. We now re-write (3.39) and (3.40) to obtain:

$$A_\ell(E,r) = \tilde{A}_\ell(E,r) - \frac{2\eta h(\eta)}{C_0^2(\eta)} C_\ell^2 k^{\ell+2}\tilde{B}_\ell(E,r) \quad (3.44)$$

$$B_\ell(E,r) = C_\ell^2 k^{\ell+2}\tilde{B}_\ell(E,r) \quad (3.45)$$

Combining (3.33) with (3.44) and (3.45) then gives the important single-channel result:

$$f_\ell^{(in/out)}(E) = \frac{e^{\mp i\sigma_\ell}}{2C_\ell(\eta)(2\ell+1)!!}\left\{\tilde{A}_\ell(E,\infty) - \left[\frac{2\eta h(\eta)}{C_0^2(\eta)} \pm i\right] C_\ell^2(\eta)k^{2\ell+1}\tilde{B}_\ell(E,\infty)\right\} \quad (3.46)$$

The above equation is the Coulombic equivalent of the equations (10) and (11) of the article [6]. We now proceed in the same way as [6], but rather than using $A_\ell(E,r)$ and $B_\ell(E,r)$ we use the holomorphic functions $\tilde{A}_\ell(E,r)$ and $\tilde{B}_\ell(E,r)$, which can be written as a power series expansion around an arbitrary point E_0

within the domain of analyticity, $\mathscr{D} \subseteq \mathbb{C}$. Note that for finite r, this domain is the entire complex plane [6], and since the Jost functions are defined for $r \to \infty$, we do not consider finite r. Thus, unfortunately, $\mathscr{D}$ is not the entire complex plane, but is centred around E_0. The point around which the expansion is done is thus very important, and has computational consequences that will be dealt with in Chapter 4. The expansions are given by:

$$\tilde{A}_\ell(E,r) = \sum_{n=0}^{\infty} \alpha_n(\ell, E_0, r)(E - E_0)^n \tag{3.47}$$

$$\tilde{B}_\ell(E,r) = \sum_{n=0}^{\infty} \beta_n(\ell, E_0, r)(E - E_0)^n \tag{3.48}$$

The coefficients, α_n and β_n will serve as the fitting parameters of the scattering data. As explained in [6] for the non-Coulomb problem, due to the fact that the coefficients can be calculated by substituting these expansions in the system of differential equations (3.41) and (3.42) with real boundary conditions (3.43), the coefficient must be real for real E_0. This is good, since the number of parameters reduces significantly. For a truncated expansion of $n = M$, there will thus be $2(M+1)$ parameters, where there would be double as many for complex E_0.

As done in [4] for the non-Coulomb problem, the expansion coefficients for Coulomb scattering can also be calculated for a known potential by solving (3.41) and (3.42). This is left for another project, though, and we concern ourselves with finding the coefficients by means of the parametrizing the scattering data, since our goal is to show that such a parametrization gives accurate results and is thus applicable to real scattering problems.

3.3 Multi-channel Coulomb scattering

3.3.1 Jost matrices for Coulomb scattering

For Coulomb scattering, the interaction operator $\mathscr{U}$ in the Hamiltonian (2.51) given in Chapter 2.3.1 will be modified by the addition of a Coulomb part H_C:

$$H = H^0 + \mathscr{U} + H_C + h \tag{3.49}$$

This results in the following system of N coupled radial differential equations for a physical system that can move in N channels, similar to (2.59):

$$\left[\partial_r^2 + k_n^2 - \frac{\ell_n(\ell_n+1)}{r^2} - \frac{2k_n\eta_n}{r}\right] u_n(E,r) = \sum_{n'=1}^{N} V_{nn'}(r)u_{n'}(E,r) \tag{3.50}$$

The extra term $\frac{2k_n\eta_n}{r}$ accounts for the long-ranged tales of the interaction. For further details, see [2]. A solution to the above system is a column $(u_1,u_2,\ldots,u_N)^T$. Each entry describes the motion in an individual channel [3]. As before, there are $2N$ linearly independent column solutions of this kind, and only half are regular for small r. The regular columns are again combined to form a square matrix, the *Fundamental Matrix of the Regular Solutions* for Coulomb scattering:

$$U(E,r) = \begin{pmatrix} u_{11}(E,r) & u_{12}(E,r) & \cdots & u_{1N}(E,r) \\ u_{21}(E,r) & u_{22}(E,r) & \cdots & u_{2N}(E,r) \\ \vdots & \vdots & \ddots & \vdots \\ u_{N1}(E,r) & u_{N2}(E,r) & \cdots & u_{NN}(E,r) \end{pmatrix} \tag{3.51}$$

Also as before, any physical solution is a linear combination of its columns [3]. As $r \to \infty$, the short-range part of (3.50) responsible for the coupling disappears, and

we are left with the following pure Coulomb system of N second order differential equations:

$$\left[\partial_r^2 + k_n^2 - \frac{\ell_n(\ell_n+1)}{r^2} - \frac{2k_n\eta_n}{r}\right] u_n(E,r) = 0, \qquad r \to \infty \tag{3.52}$$

Because $r \to \infty$, there is no condition for regularity, and there are thus $2N$ possible linearly-independent column solutions [3], which form a basis in the solution space. Naturally, there are many choices for this basis, but it is convenient, because they are reasonably well-studied, to choose solutions in terms of the Regular and Irregular Coulomb functions, $F_\ell(\eta,kr)$ and $G_\ell(\eta,kr)$:

$$F(E,r) = \begin{pmatrix} F_{\ell_1}(\eta_1,k_1r) & 0 & \cdots & 0 \\ 0 & F_{\ell_2}(\eta_2,k_2r) & \cdots & 0 \\ \vdots & \vdots & \ddots & \vdots \\ 0 & 0 & \cdots & F_{\ell_N}(\eta_N,k_Nr) \end{pmatrix} \tag{3.53}$$

$$G(E,r) = \begin{pmatrix} G_{\ell_1}(\eta_1,k_1r) & 0 & \cdots & 0 \\ 0 & G_{\ell_2}(\eta_2,k_2r) & \cdots & 0 \\ \vdots & \vdots & \ddots & \vdots \\ 0 & 0 & \cdots & G_{\ell_N}(\eta_N,k_Nr) \end{pmatrix} \tag{3.54}$$

The matrices of the Coulomb spherical waves are then given by the linear combinations:

$$H^{(\pm)}(E,r) = F(E,r) \mp iG(E,r) \tag{3.55}$$

If $\eta = 0$, the matrices $H^{(\pm)}$ simply become the matrices $W^{(in/out)}$ of equations (2.65) and (2.66). As is done by Rakityansky [3], by analogy with (3.5), the following is postulated for the fundamental matrix (3.51) since $F(E,r)$ and $G(E,r)$

are solutions at large r:

$$U(E,r) = F(E,r)A(E,r) + G(E,r)B(E,r) \tag{3.56}$$

When this is substituted into the radial Coulomb Schrödinger equation, (3.50), the following differential equations for $A(E,r)$ and $B(E,r)$ are obtained [3] (the functional dependence is suppressed to facilitate ease of reading):

$$\partial_r A = K^{-1}GV\,(FA+GB) \tag{3.57}$$

$$\partial_r B = -K^{-1}FV\,(FA+GB) \tag{3.58}$$

Where V and K are given by:

$$V = V_{nn'}(r) \tag{3.59}$$

$$K = \begin{pmatrix} k_1 & 0 & \cdots & 0 \\ 0 & k_2 & \cdots & 0 \\ \vdots & \vdots & \ddots & \vdots \\ 0 & 0 & \cdots & k_N \end{pmatrix} \tag{3.60}$$

The boundary conditions of (3.57) and (3.58) are given by:

$$A(E,0) = I, \qquad B(E,0) = 0 \tag{3.61}$$

This follows from the fact that $U(E,r)$ must be regular at $r = 0$: By definition, $F(E,r)$ is regular and $G(E,r)$ is irregular. From equation (3.56) it can be seen that $U(E,r)$ can only be regular at the origin if $G(E,r)$ is suppressed, which results in

the second of the boundary conditions. $A(E,0)$ can of course be any constant matrix, but we choose the identity matrix for simplicity and worry about normilization later (or not, as explained at the end of Chapter 2.2.3). At the origin, $U(E,r)$ thus becomes:

$$U(E,r) \xrightarrow[r\to 0]{} F(E,r) = \begin{pmatrix} F_{\ell_1}(\eta_1,k_1r) & 0 & \cdots & 0 \\ 0 & F_{\ell_2}(\eta_2,k_2r) & \cdots & 0 \\ \vdots & \vdots & \ddots & \vdots \\ 0 & 0 & \cdots & F_{\ell_N}(\eta_N,k_Nr) \end{pmatrix}$$

$$\xrightarrow[r\to 0]{} \begin{pmatrix} C_{\ell_1}(\eta_1)(k_1r)^{\ell_1+1} & 0 & \cdots & 0 \\ 0 & C_{\ell_2}(\eta_2)(k_2r)^{\ell_2+1} & \cdots & 0 \\ \vdots & \vdots & \ddots & \vdots \\ 0 & 0 & \cdots & C_{\ell_N}(\eta_N)(k_Nr)^{\ell_N+1} \end{pmatrix}$$

$$\therefore U(E,r) \xrightarrow[r\to 0]{} C \begin{pmatrix} (k_1r)^{\ell_1+1} & 0 & \cdots & 0 \\ 0 & (k_2r)^{\ell_2+1} & \cdots & 0 \\ \vdots & \vdots & \ddots & \vdots \\ 0 & 0 & \cdots & (k_Nr)^{\ell_N+1} \end{pmatrix} \tag{3.62}$$

with C given in terms of the Coulomb barrier function by:

$$C = \begin{pmatrix} C_{\ell_1} & 0 & \cdots & 0 \\ 0 & C_{\ell_2} & \cdots & 0 \\ \vdots & \vdots & \ddots & \vdots \\ 0 & 0 & \cdots & C_{\ell_N}(\eta_N) \end{pmatrix}$$

We now consider the fundamental matrix of regular solutions, Φ, the N columns of which form the basis of regular solutions to equation(3.52), as (2.62) does for

the non-Coulomb case in Chapter 2.3.1.

As with the single channel Coulomb scattering, the matrix $\Phi(E,r)$ and $U(E,r)$ differ by a constant factor:

$$\begin{aligned}\Phi(E,r) &= C^{-1}L^{-1}U(E,r) \qquad (3.63)\\ &\xrightarrow[r\to 0]{} \begin{pmatrix} j_{\ell_1}(,k_1r) & 0 & \cdots & 0 \\ 0 & j_{\ell_2}(,k_2r) & \cdots & 0 \\ \vdots & \vdots & \ddots & \vdots \\ 0 & 0 & \cdots & j_{\ell_N}(k_Nr) \end{pmatrix}\end{aligned}$$

with L given by:

$$L = \begin{pmatrix} (2\ell_1+1)!! & 0 & \cdots & 0 \\ 0 & (2\ell_2+1)!! & \cdots & 0 \\ \vdots & \vdots & \ddots & \vdots \\ 0 & 0 & \cdots & (2\ell_N+1)!! \end{pmatrix} \qquad (3.64)$$

Note that '!!' refers to the double factorial, defined as:

$$(2k-1)!! = \prod_{n=1}^{k}(2n-1), \qquad \forall k,n \in \mathbb{N} \qquad (3.65)$$

Now, the matrix $\Phi(E,r)$ is used to define the Jost matrices for Coulomb scattering. At large distances, it can be written as a linear combination of the $2N$ columns of the basis $H^{(-)}$ and $H^{(+)}$:

$$\Phi(E,r) \xrightarrow[r\to\infty]{} H^{(-)}(E,r)\sigma^{(+)}f^{(in)}(E) + H^{(+)}(E,r)\sigma^{(-)}f^{(out)}(E) \qquad (3.66)$$

with:

$$\sigma^{(\pm)} = \begin{pmatrix} e^{\pm i\sigma_{\ell_1}} & 0 & \cdots & 0 \\ 0 & e^{\pm i\sigma_{\ell_2}} & \cdots & 0 \\ \vdots & \vdots & \ddots & \vdots \\ 0 & 0 & \cdots & e^{\pm i\sigma_{\ell_N}} \end{pmatrix} \tag{3.67}$$

Now we introduce the linear combination of the unknown matrices $A(E,r)$ and $B(E,r)$:

$$\mathscr{F}^{(in/out)}(E,r) = \frac{1}{2}\left[A(E,r) \mp iB(E,r)\right] \tag{3.68}$$

From (3.56) this results in:

$$U(E,r) = H^{(-)}(E,r)\mathscr{F}^{(in)}(E,r) + H^{(+)}(E,r)\mathscr{F}^{(out)}(E,r) \tag{3.69}$$

$$\xrightarrow[r\to\infty]{} H^{(-)}(E,r)\mathscr{F}^{(in)}(E,\infty) + H^{(+)}(E,r)\mathscr{F}^{(out)}(E,\infty) \tag{3.70}$$

Therefore, the Jost Matrices are given by:

$$f^{(in/out)}(E) = \lim_{r\to\infty} C^{-1}L^{-1}\sigma^{(\mp)}\mathscr{F}^{(in/out)}(E,r) \tag{3.71}$$

Of course we now need to show how $A(E,r)$ and $B(E,r)$ can be written so that the k- and η-dependence is factorised. An interesting question is why we factorise the k- and η-dependence of $A(E,r)$ and $B(E,r)$, and then use the power-series expansion parameters of these functions in stead of working directly with the matrices $\mathscr{F}^{(in/out)}(E,r)$.

In fact, there is no reason we could not do this. Historically we rather use $A(E,r)$ and $B(E,r)$, since, if the potential is known, calculating these two matrices numerically is easier because the matrix elements are oscillatory in nature, where the matrix elements of $\mathscr{F}^{(in/out)}(E,r)$ are exponential in nature. Also, the his-

torical effective range expansion parameters like scattering length and effective radius can easily be determined from $A(E,r)$ and $B(E,r)$ [3]. We thus carry on in the same vein.

3.3.2 Analytic structure of Jost matrices

We now construct the following diagonal matrices according to [20] as done by [3]:

$$D = \begin{pmatrix} C_{\ell_1}(\eta_1)k_1^{\ell_1+1} & 0 & \cdots & 0 \\ 0 & C_{\ell_2}(\eta_2)k_2^{\ell_2+1} & \cdots & 0 \\ \vdots & \vdots & \ddots & \vdots \\ 0 & 0 & \cdots & C_{\ell_N}(\eta_N)k_N^{\ell_N+1} \end{pmatrix} \tag{3.72}$$

$$M = \begin{pmatrix} \frac{2\eta_1 h(\eta_1)}{C_0^2(\eta_1)} & 0 & \cdots & 0 \\ 0 & \frac{2\eta_2 h(\eta_2)}{C_0^2(\eta_2)} & \cdots & 0 \\ \vdots & \vdots & \ddots & \vdots \\ 0 & 0 & \cdots & \frac{2\eta_N h(\eta_N)}{C_0^2(\eta_N)} \end{pmatrix} \tag{3.73}$$

From which we obtain the following entire functions of E:

$$\tilde{A} = DAD^{-1} + MDBD^{-1} \tag{3.74}$$

$$\tilde{B} = KD^{-1}BD^{-1} \tag{3.75}$$

This is a generalization of the single-channel functions, (3.44) and (3.45), and all attributes pertaining to the single-functions are applicable to the matrices: they are analytic single-valued functions of E within the domain $\mathscr{D}$ along the real positive

axis [3]. Substitution of (3.74) and (3.75) into (3.68) then gives the following result for the Jost matrices:

$$f^{(in/out)}(E) = \frac{1}{2}C^{-1}L^{-1}\sigma^{(\mp)}\lim_{r\to\infty}\left[D^{-1}\tilde{A}D - (M \pm i)K^{-1}D\tilde{B}D\right] \tag{3.76}$$

The matrix elements are then given by:

$$f^{(in/out)}(E) = \frac{e^{\pi\eta_m/2}\ell_m!}{2\Gamma(\ell_m+1\pm i\eta_m)}\left\{\frac{C_{\ell_n}(\eta_n)k_n^{\ell_n+1}}{C_{\ell_m}(\eta_m)k_m^{\ell_m+1}}\tilde{A}_{mn}(E,\infty)\right. \tag{3.77}$$

$$\left. - \left[\frac{2\eta_m h(\eta_m))}{C_0^2(\eta_m)} \pm i\right] C_{\ell_m}(\eta_m)C_{\ell_n}(\eta_n)k_m^{\ell_m}k_n^{\ell_n+1}\tilde{B}_{mn}(E,\infty)\right\}$$

For $m,n = 1,2,...,N$. Thus, similar to the single channel result, the Jost matrices are expressed in terms of the single valued and analytic functions of energy, $\tilde{A}_\ell(E,r)$ and $\tilde{B}_\ell(E,r)$, with the k- and η dependence effectively isolated. Also, if $m = n = 1$, it is easy to see that the single-channel result, equation (3.46) is retrieved. The power-series expansion around E_0 is then also given by:

$$\tilde{A}_\ell(E,r) = \sum_{n=0}^{\infty}\alpha_n(\ell,E_0,r)(E-E_0)^n \tag{3.78}$$

$$\tilde{B}_\ell(E,r) = \sum_{n=0}^{\infty}\beta_n(\ell,E_0,r)(E-E_0)^n \tag{3.79}$$

Where the parameters α_n and β_n are $N\times N$ matrices.

Chapter 4

Fitting procedure

4.1 Fitting parameters

Equations (3.47) and (3.48) are identical to equations (3.78) and (3.79), where $\tilde{A}_\ell(E,r), \tilde{B}_\ell(E,r), \alpha_n(\ell,E_0,r)$ and $\beta_n(\ell,E_0,r)$ simply become $N \times N$ matrices for multi-channel scattering. The expansion will of course be truncated to $n = M$ terms:

$$\tilde{A}_\ell(E,r) \approx \sum_{n=0}^{M} \alpha_n(\ell,E_0,r)(E-E_0)^n \tag{4.1}$$

$$\tilde{B}_\ell(E,r) \approx \sum_{n=0}^{M} \beta_n(\ell,E_0,r)(E-E_0)^n \tag{4.2}$$

This then means there will be $2(M+1)N^2$ fitting parameters, where M is the highest power in the expansion, and N is the number of channels. As indicated before, if E_0 was chosen to be complex, this number would double, since there would be an unknown real and imaginary part to each parameter, not only just a real part.

The approximate expressions (4.1) and (4.2) can only be accurate within a circle

around E_0 [6]. The choice of E_0 should thus firstly be real, and secondly close to the expected resonance. Thus, a value close to the peak in the scattering data should be suitable. Also, the more terms taken (larger M), the wider the circle, as indicated in [15]. Unfortunately, it is computationally absurd to choose too large a value for M. If $M = 12$ for a 2-channel problem, for example, we would have 104 parameters to fit. It turns out suitable accuracy is, thankfully, obtained for $M = 5$; provided E_0 is suitably close to the resonance value.

4.2 Single-channel scattering

For single-channel scattering, the fitting procedure is quite simple. We have the following set of scattering data:

$$\sigma(E_i) \pm \delta_i, \qquad i = 1,2,3,\ldots,N$$

Where $\sigma(E)$ is the cross-section at a specific energy, E, with corresponding standard deviation δ. See, for example, Figure 5.1. The energies, E, are in an interval around the point E_0 where a resonance is expected. We now construct the function χ^2, which is to be minimized, as follows:

$$\chi^2 = \sum_{i=1}^{N} \left[\frac{\sigma(E_i) - \sigma^{fit}(E_i)}{\delta_i} \right]^2 \tag{4.3}$$

It is clear that the function χ^2 will be a minimum when the fitted cross section, $\sigma^{fit}(E)$, is equal to the true cross section $\sigma(E)$. The fitted cross section is given

in terms of the Jost functions by equation (2.50):

$$\sigma^{fit}(E) = \sum_{\ell} \frac{\pi}{k^2}(2\ell+1)\left|\frac{f_\ell^{(out)}(E)}{f_\ell^{(in)}(E)} - 1\right|^2$$

Where the Jost functions $f_\ell^{(in/out)}(E)$ are given by (3.46), together with equations (4.1) and (4.2) so that the fitting parameters are α_n and β_n.

The function χ^2 given by (4.3) is minimized with the *Minuit* code in Fortran [21]. There are other equally powerful and effective codes available, but *Minuit* proves more than adequate for our purposes. Also, there is much information and support available for the program, since it is an older code. Different values for the 12 single-channel parameters (if $m = 5$) are randomly generated, implemented in *Minuit*, and a minimum of χ^2 is found. Roughly 1000 sets of random choices of the starting values for the parameters are implemented, and the adjusted set giving the best minimum corresponds with the correct parameters.

4.3 Two-channel scattering

We follow the same fitting procedure as outlined in [6], with $N = 2$. It is also simply an extension of single-channel scattering. Suppose we have a set of experimental data for two-channel scattering; $1 \to 1$, $1 \to 2$, $2 \to 1$, and $2 \to 2$:

$$\sigma_{1,1}\left(E_{i_1}^{(1,1)}\right) \pm \delta_{i_1}^{(1,1)}, \qquad i_1 = 1,2,3,\ldots,N^{(1,1)}$$

$$\sigma_{1,2}\left(E_{i_2}^{(1,2)}\right) \pm \delta_{i_2}^{(1,2)}, \qquad i_2 = 1,2,3,\ldots,N^{(1,2)}$$

$$\sigma_{2,1}\left(E_{i_3}^{(2,1)}\right) \pm \delta_{i_3}^{(2,1)}, \qquad i_3 = 1,2,3,\ldots,N^{(2,1)}$$

$$\sigma_{2,2}\left(E_{i_4}^{(2,2)}\right) \pm \delta_{i_4}^{(2,2)}, \qquad i_4 = 1,2,3,\ldots,N^{(2,2)}$$

See for example Figure 5.5 and Figure 5.6. The function to be minimized, χ^2, is then constructed as follows:

$$\begin{aligned}\chi^2 = &\sum_{i_1=1}^{N^{(1,1)}} \left[\frac{\sigma_{1,1}\left(E_{i_1}^{(1,1)}\right) - \sigma_{1,1}^{fit}\left(E_{i_1}^{(1,1)}\right)}{\delta_{i_1}^{(1,1)}}\right]^2 \\ &+ \sum_{i_2=1}^{N^{(1,2)}} \left[\frac{\sigma_{1,2}\left(E_{i_2}^{(1,2)}\right) - \sigma_{1,2}^{fit}\left(E_{i_2}^{(1,2)}\right)}{\delta_{i_2}^{(1,2)}}\right]^2 \\ &+ \sum_{i_3=1}^{N^{(2,1)}} \left[\frac{\sigma_{2,1}\left(E_{i_3}^{(2,1)}\right) - \sigma_{2,1}^{fit}\left(E_{i_3}^{(2,1)}\right)}{\delta_{i_3}^{(2,1)}}\right]^2 \\ &+ \sum_{i_4=1}^{N^{(2,2)}} \left[\frac{\sigma_{2,2}\left(E_{i_4}^{(2,2)}\right) - \sigma_{2,2}^{fit}\left(E_{i_4}^{(2,2)}\right)}{\delta_{i_4}^{(2,2)}}\right]^2 \\ &+ \sum_j |S_{1,2}(E_j) - S_{2,1}(E_j)|\end{aligned} \tag{4.4}$$

The first four terms account for the comparison between a data point and a fitted point and ensures that the fitted point equals the data point, as with single channel scattering. The last term, on the other hand, ensures the required symmetry of the S-matrix [6]; which is not necessarily guaranteed when the function is minimised without this term.

The fitted partial-wave cross section is calculated by equation (2.70) from Chapter 2:

$$\sigma_{mn}^{fit}(E) = \frac{\pi}{k_m^2}(2\ell_m + 1)\,|S_{nm}(E) - \delta_{mn}|^2$$

with, as was shown:

$$S(E) = f^{(out)}(E)\left[f^{(in)}(E)\right]^{-1}$$

And of course the functions $f^{(in/out)}(E)$ given by equation (3.77), with (4.1) and (4.2), so that the fitting parameters are the matrix elements of α_n and β_n.

The function χ^2 given by (4.4) is also minimized with the *Minuit* code in Fortran in exactly the same way as with the single-channel problem, except that there will be 48 parameters (N=1, m=5) instead of 12.

Chapter 5

Examples

5.1 Single-channel model

The purpose of this work is to show that the method of extracting resonance parameters outlined in the previous chapters is practical, and gives sufficiently accurate results. To this end, a known potential is used in the system of differential equations (3.6) and (3.7), to determine the functions $A_\ell(E,r)$ and $B_\ell(E,r)$. These are then used to determine the Jost functions, with equations (3.33), from which the resonances are located, as shown in Chapter 2. Also, with the Jost functions known, the actual scattering cross sections in any energy-range can easily be determined with equations (2.50). Thus the exact Jost functions allows pseudo data-points to be generated around energies where resonances occur, which will serve as the experimental data points.

In performing calculations, the units are chosen such that $\hbar/\mu = 1$ (atomic units). Thus energies and distances will be dimensionless [6]. The Sommerfield parameter, η, is already dimensionless. We could just as easily have chosen $c = \varepsilon_0 = \mu_0 = 1$, with energies in MeV and distances in fm. The same values

would be obtained.

The potential we will use is the well-studied Noro-Taylor potential with an added Coulomb tail, as used by Sofianos and Rakityansky in the paper [5]. As stated by them, this choice of potential is,

"...motivated by the richness of the spectra generated by these potentials, and their simple form."

The potential is given by:

$$V(r) = 7.5r^2e^{-r} + \frac{2k\eta}{r} \tag{5.1}$$

The short-range part of the potential is given by the first term. The Sommerfield parameter, η, is given by equation (3.2) as before. For this example, we chose η in such a way that:

$$\begin{aligned} 2k\eta &= -1 \\ \therefore \eta &= \frac{-1}{2k} \end{aligned} \tag{5.2}$$

We also choose $\ell = 0$, for simplicity. In determining the exact Jost functions, complex rotation is implemented, as shown in [15]. The exact resonances are given in Table 5.1.

	E_r (Calculated)	Γ (Calculated)	E_r (Literature)	Γ (Literature)
1	1.780524536	0.000095719	1.780524536	0.000095719
2	4.101494946	1.157254428	4.101494946	1.157254428
3	4.663461095	5.366401541	4.663461099	5.366401539

Table 5.1: The exact resonance energies and widths of the first three resonances generated by potential (5.1), compared with results from [5].

The results compare favourably with the literature, except for the third resonance where there is insignificant deviation, probably caused by differences in the code generating the somewhat fickle Regular and Irregular Coulomb functions, $F_\ell(\eta,kr)$ and $G_\ell(\eta,kr)$.

Two sets of data points are then generated for different energy intervals, around the first and second resonances. These are given in Figure 5.1 and Figure 5.2. Each set contains 15 data points. The plots of the fitted data are given by Figure 5.3 and Figure 5.4. The sharp peak that appears in the fitted data of the first plot, is due to a lack of sufficient data points in that interval. It is not too close to the actual resonance peak, and does not negatively influence the result of the first resonance.

From the first plot, the first resonance is obtained, and from the second plot, the second and third resonances are obtained. The values of the resonances, together with the exact values, are given in Table 5.2.

	E_r (Fit)	Γ (Fit)	E_r (Exact)	Γ (Exact)
1	1.780522312	0.000096468	1.780524536	0.000095719
2	4.101337806	1.15539920	4.101494946	1.157254428
3	4.555463672	3.588071237	4.663461095	5.366401541

Table 5.2: The resonance energies and widths obtained from parametrizing the data generated by the potential (5.1), together with the exact resonance energies and widths generated by the same potential.

Sufficient accuracy is obtained for the first and second resonance, but the third resonance proves problematic. The resonance width is rather large, which does make it difficult to accurately determine, since it is far from the real axis in the Argand plane [6]. Possibly more accuracy would have been obtained if there had been more data points around the third resonance, but since we only really set out to determine the first two resonances, this is not required.

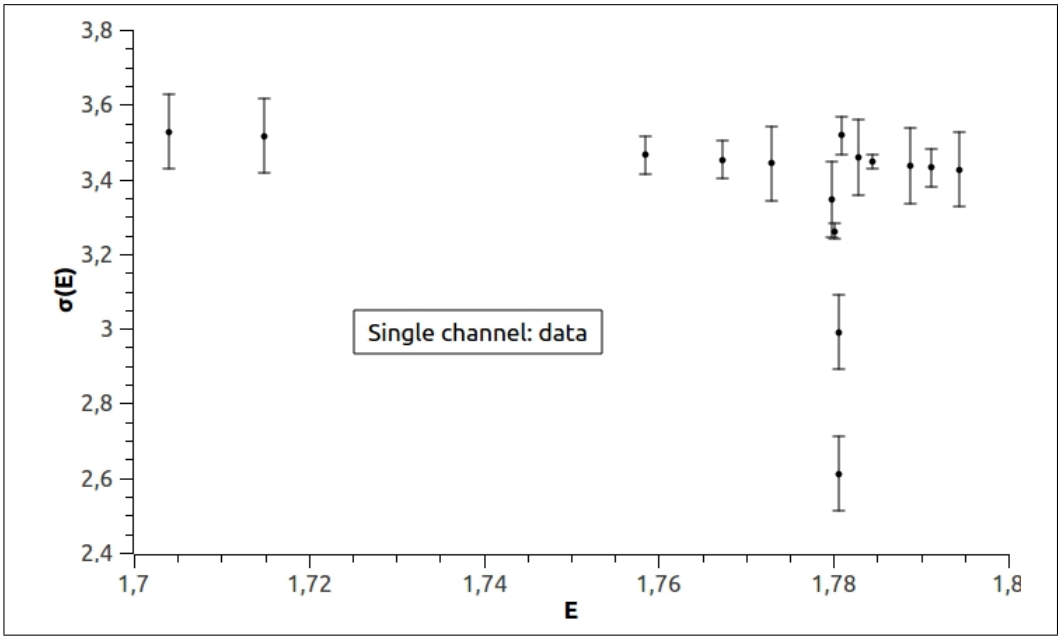

Figure 5.1: Artificial data points for the single-channel model (5.1) for $1.7 \leq E \leq 1.8$.

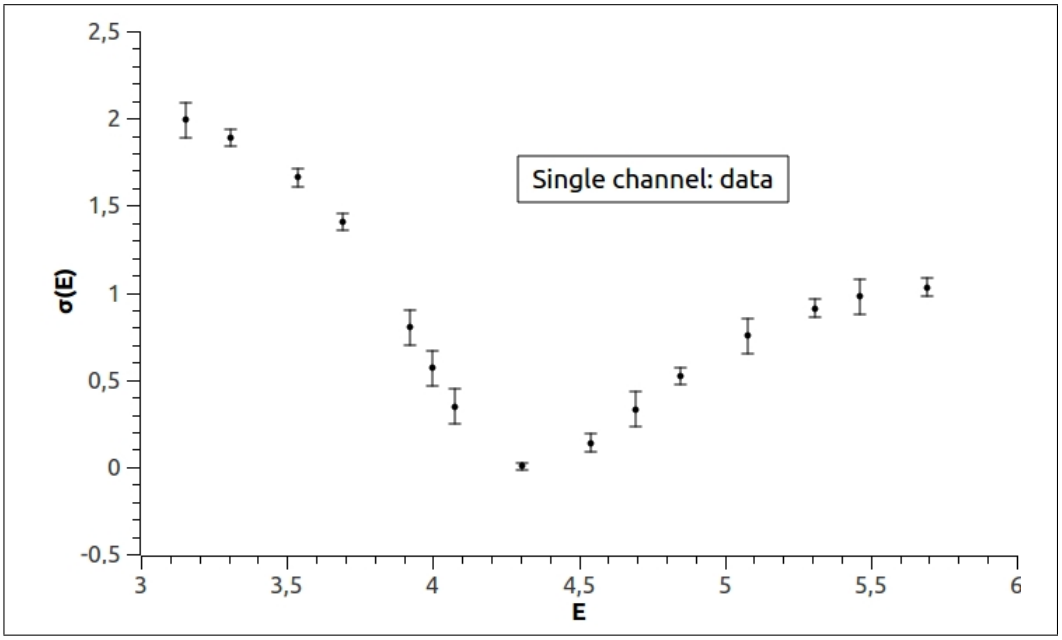

Figure 5.2: Artificial data points for the single-channel model (5.1) for $3.0 \leq E \leq 6.0$.

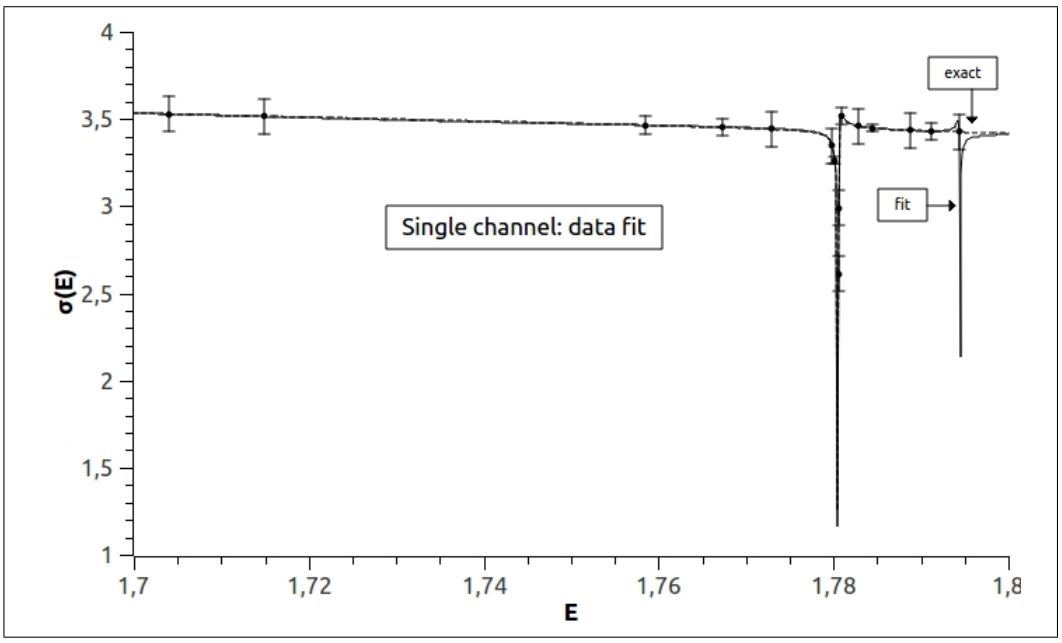

Figure 5.3: Exact cross section (dashed curve) for the single-channel model (5.1) and the result of fitting the data (thick curve) with $M = 5$ and $E_0 = 1.7$ in equations (4.1) and (4.2) for $1.7 \leq E \leq 1.8$.

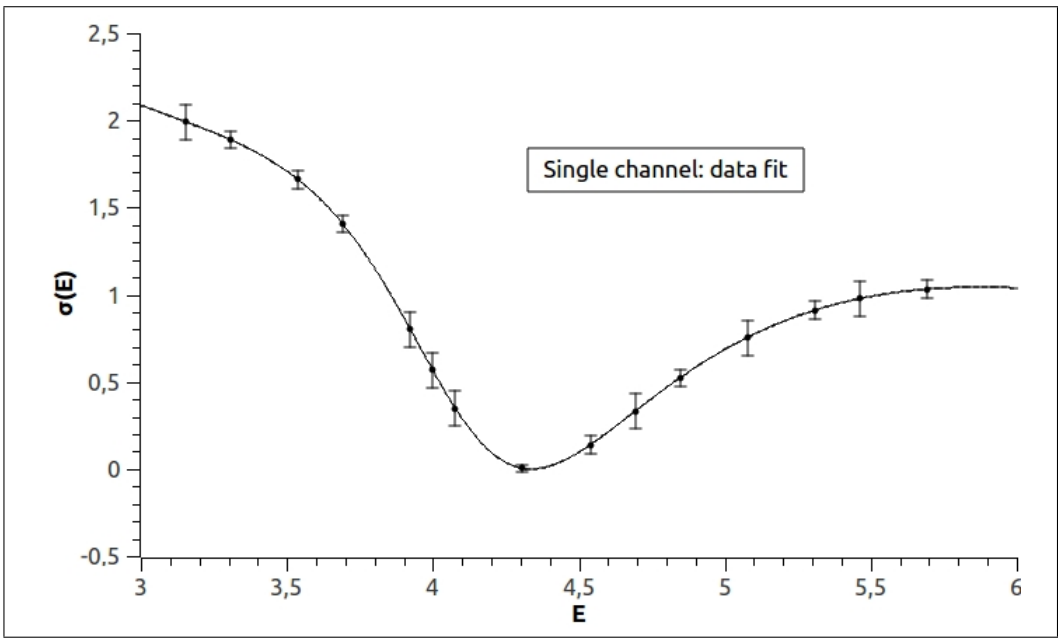

Figure 5.4: Exact cross section (dashed curve) for the single-channel model (5.1) and the result of fitting the data (thick curve) with $M = 5$ and $E_0 = 4.0$ in equations (4.1) and (4.2) for $3.0 \leq E \leq 6.0$.

5.2 Two-channel model

The potential used is given by:

$$V(r) = \begin{pmatrix} -1.0 & -7.5 \\ -7.5 & 7.5 \end{pmatrix} r^2 e^{-r} + \begin{pmatrix} 1 & 0 \\ 0 & 1 \end{pmatrix} \frac{2k\eta}{r} \tag{5.3}$$

This is clearly simply the two-channel Noro-Taylor potential with an added Coulomb tail. For this example we choose:

$$\begin{aligned} 2k\eta &= 1 \\ \therefore \eta &= \frac{1}{2k} \end{aligned} \tag{5.4}$$

Thus the potential is repulsive, as opposed to the single-channel example where it was attractive. In theory, we could easily consider an attractive potential again, but possible complications arise that need to be taken into account, as explained in [3]. For all channels, $\ell = 0$. The exact resonances are obtained, and are given in Table 5.4. The partial widths are given by Γ_1 and Γ_2, and are determined as outlined in [6].

Figure 5.5 and Figure 5.6 show the pseudo-data points generated for the elastic scattering $1 \to 1$ and $2 \to 2$ respectively, each containing 25 data points in the interval $6 \leq E \leq 11$. Fewer data points give unsatisfactory results. Roughly 5000 sets of random starting values of the parameters are then implemented in *Minuit*, and the expansion is done around the real energy $E_0 = 8$. Figure 5.7 and Figure 5.8 show the result of the data-fit. Figure 5.9 and 5.10 show the predicted cross sections for $1 \to 2$ and $2 \to 1$, for which no pseudo-data points were generated, and thus no fit was possible.

It seems that the results of the fit all show an incorrect peak around $E = 9.5$. This is once again due to a lack of sufficient data points around this energy. If this method were applied to a real scattering problem, one might be concerned that one would find similar incorrect resonance peaks when fitting the scattering data. Yet it is easy to see that, if the experimental data points do not show a peak in a specific energy interval, the fitted data should not either, and any resonances parameters obtained around such an incorrect peak should be ignored.

Apart from this anomaly, the $1 \to 1$ and $2 \to 2$ fits are almost exact, and the predictions for $1 \to 2$ and $2 \to 1$ agree with the exact plots quite admirably around the the first resonance, and definitely reflects the general trend of the data elsewhere. This is quite remarkable, if one considers that no data was available in these channels. The resonances obtained from the fit are given in Table 5.3. Note that all resonances are obtained by finding the zeros of the appropriate Jost matrix determinant by making use of the Newton-Raphson method, although any suitable numerical method would suffice.

The first resonance corresponds very well with the exact values. For the second resonance, already significantly wide, sufficient accuracy is obtained. The third and fourth resonances are completely off, unfortunately, but this is understandable for three reasons: firstly, as noted before, wider resonances are difficult to determine. Secondly, the unfortunate sharp peak at $E = 9.5$ has skewed the results around that energy. With more data points, greater accuracy might be attainable. Thirdly, if the expansion was done around a point closer to the third or fourth resonance, $E_0 = 9$ for example, we would certainly achieve reasonable values; as indicated by [6].

Interestingly, if data points in the interval $7 \leq E \leq 11$ around the second resonance are taken and parametrized, excluding data points around the first resonance, the resulting resonance values from the fit are very unsatisfactory, specifically the

second resonance values (obviously, no value for the first resonance is obtained). Also, the predictions for cross sections of transition processes $1 \rightarrow 2$ and $2 \rightarrow 1$ do not reflect the correct trend at all. Only when data points in the interval $6 \leq E \leq 11$ around the first resonances are used as well, in other words including the first sharp peak, do we manage to determine the second resonance sufficiently accurately.

This is partially in contradiction with [6], where it is specifically noted that:

"We therefore should not fit the data within a too wide energy-interval. The central point E_0 must be placed somewhere in the middle of the interval where it is expected to find a resonance."

It seems that in dealing with wider resonances, wider energy intervals are required. As was seen with the single-channel problem, on the other hand, a very small energy interval with sufficient data points is quite suitable to locate a sharp resonance. In fact, initially, a much wider interval was used to attempt to find the first resonance of the single-channel model, but this did not result in sufficient accuracy.

We may risk amending the above quote by saying wider energy-intervals are permitted, especially with wide resonances, provided that there are sufficiently many data points in the interval. A total of 50 data points was required to accurately determine the first two resonances for the two-channel problem. Fewer data points resulted in considerably less accuracy, and more data-points would presumably cause greater accuracy, possibly even enabling the correct calculation of the wider resonances. Of course, more data points causes a marked increase in computing time - there is much more data to fit.

The fact that E_0 must still be placed close enough to a resonance is still fundamentally important, though. Unfortunately, there is no way to determine a sufficiently close E_0 value except by trial-and-error. The general shape of the scattering data

can assist, though, since resonances mostly occur around peaks in the data, as indicated before The energy around which a peak occurs, would thus be a good starting value for E_0, although many different values should be tried. Of course, in these examples, we are fortunate to *know* what the resonances are, thus we could easily choose a value for E_0 sufficiently close to the real part of the exact resonance value.

	E_r	Γ	Γ_1	Γ_2
1	6.278077399	0.036743077	0.006911563	0.029831514
2	8.036853176	2.308208500	0.370340464	1.937868036
3	9.278851942	3.534725883	1.026275547	2.508450336
4	10.73567982	7.764850961	1.576717241	6.188133719

Table 5.3: The resonance energies and widths obtained from parametrizing the data generated by the potential (5.3).

	E_r	Γ	Γ_1	Γ_2
1	6.278042551	0.036866729	0.006898807	0.029967922
2	8.038507867	2.563111275	0.617710684	1.945400591
3	8.861433400	7.883809113	1.949506410	5.934302704
4	9.020824224	14.07907263	3.591961102	10.48711153
5	8.566130944	20.75266055	5.414178669	15.33848188
6	7.548492959	27.69926473	7.328979882	20.37028485

Table 5.4: The resonance energies and widths generated by the potential (5.3).

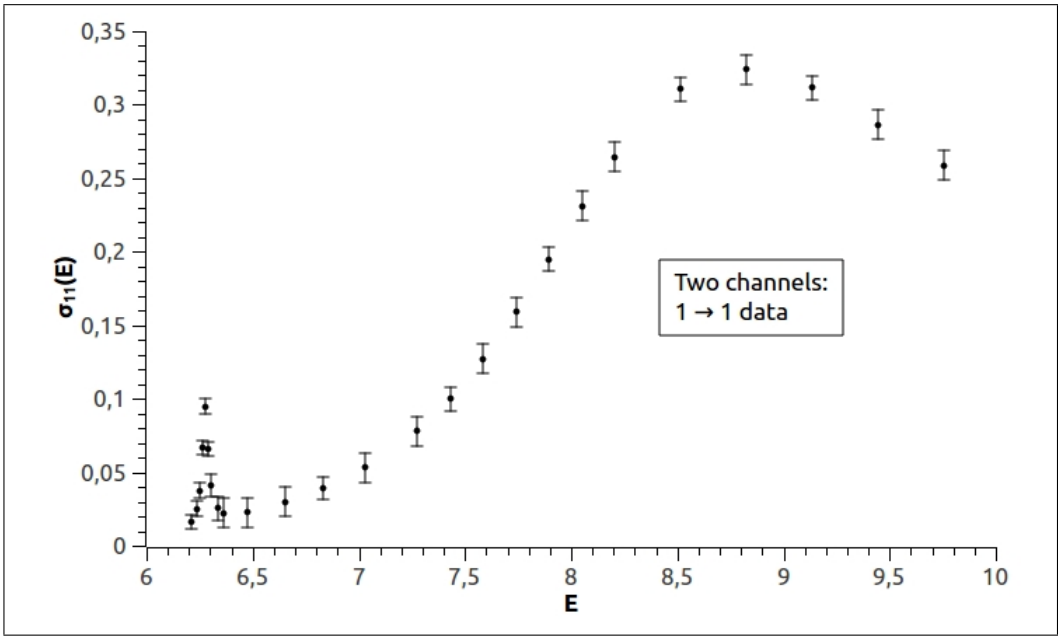

Figure 5.5: Artificial data points for the first elastic channel of the model (5.3).

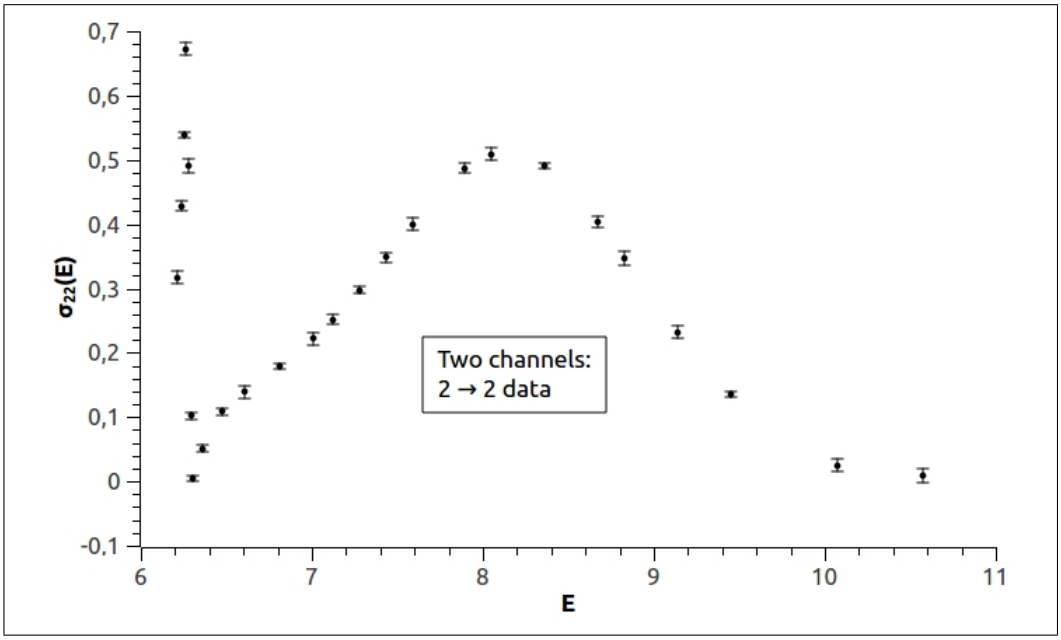

Figure 5.6: Artificial data points for the second elastic channel of the model (5.3).

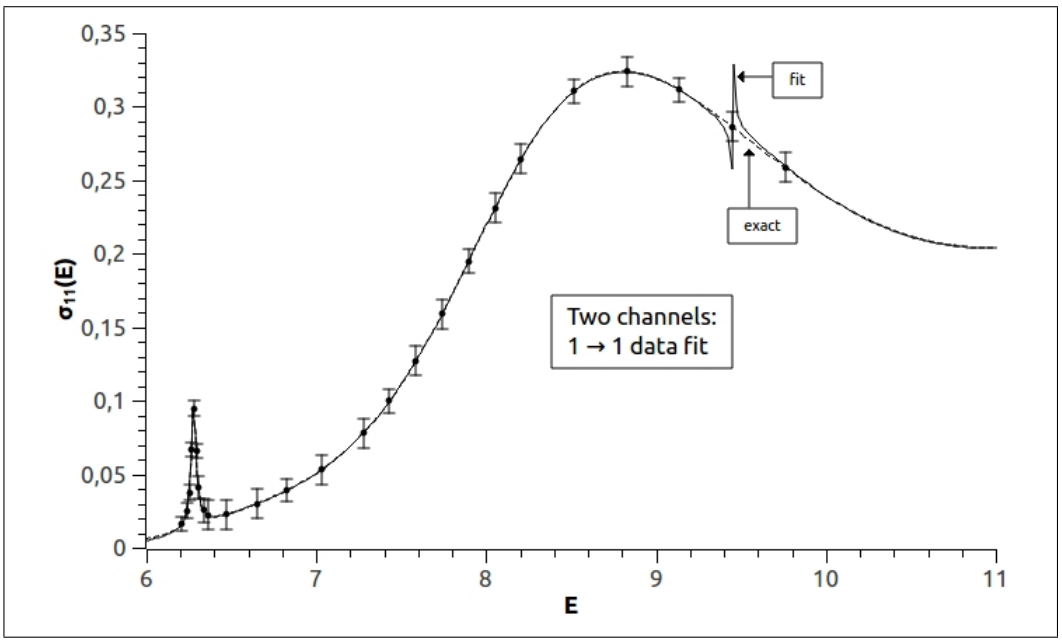

Figure 5.7: Exact elastic cross section $1 \to 1$ (dashed curve) for the two-channel model (5.3) and the result of fitting of the data (thick curve) with $M = 5$ and $E_0 = 8.0$ in equations (4.1) and (4.2).

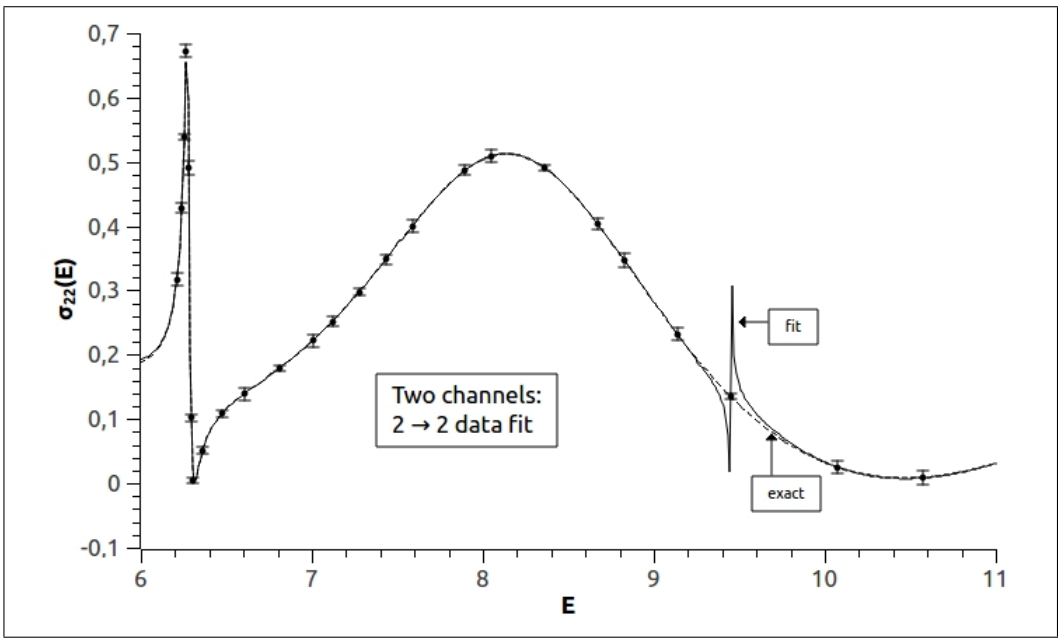

Figure 5.8: Exact elastic cross section $2 \to 2$ (dashed curve) for the two-channel model (5.3) and the result of fitting of the data (thick curve) with $M = 5$ and $E_0 = 8.0$ in equations (4.1) and (4.2).

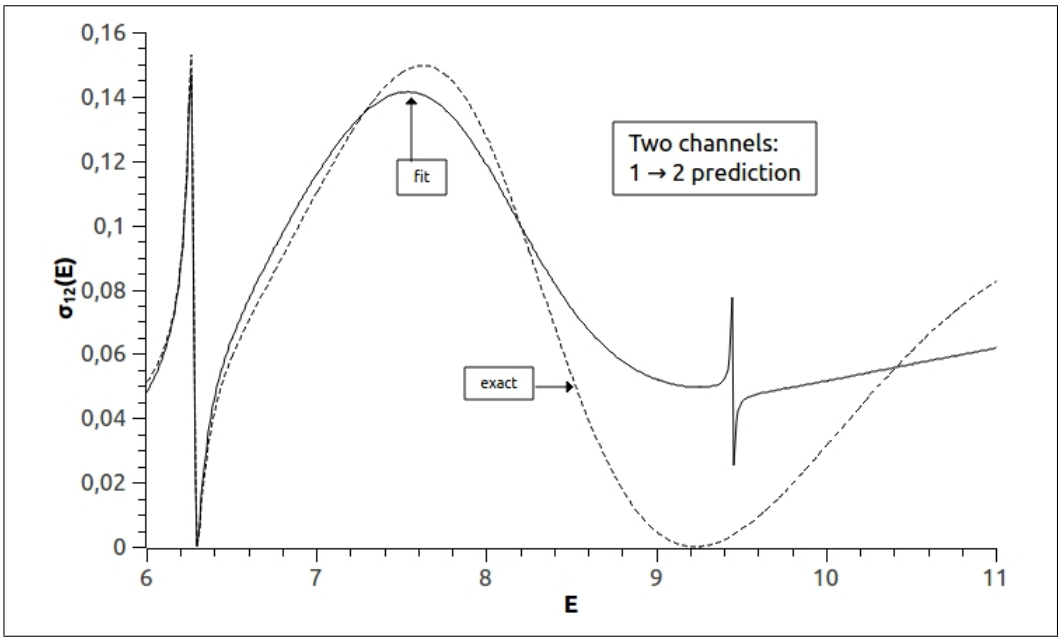

Figure 5.9: Exact elastic cross section $1 \to 2$ (dashed curve) for the two-channel model (5.3) and the prediction (thick curve) based on fitting of the data in the energy interval $6 \leq E \leq 11$ in the elastic channels $1 \to 1$ and $2 \to 2$ with $M = 5$ and $E_0 = 8.0$ in equations (4.1) and (4.2).

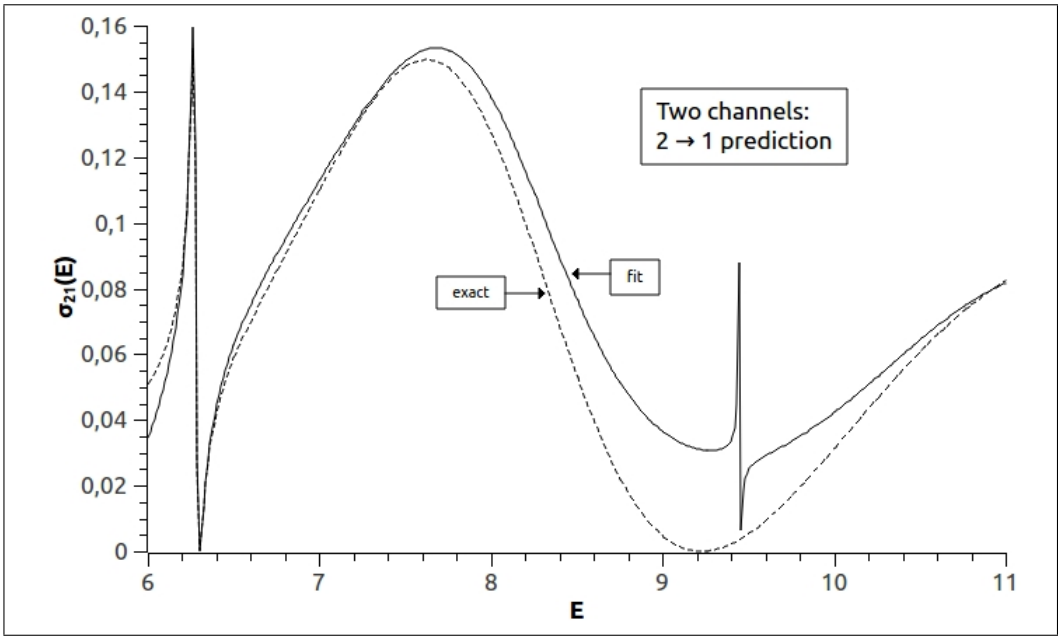

Figure 5.10: Exact elastic cross section $2 \to 1$ (dashed curve) for the two-channel model (5.3) and the prediction (thick curve) based on fitting of the data in the energy interval $6 \leq E \leq 11$ in the elastic channels $1 \to 1$ and $2 \to 2$ with $M = 5$ and $E_0 = 8.0$ in equations (4.1) and (4.2).

Chapter 6

Conclusion

This work is based on writing the Regular and Irregular Coulomb functions in terms of a holomorphic and non-holomorphic part, as done by Lambert [20]. This separation is implemented by Rakityansky [3] in the single- and multi-channel Jost matrices for a system where both short- and long-ranged interactions are present.

In this way, the channel-momenta, k_n, and the Sommerfield parameters, η_n, are factorised in the expressions obtained for the Jost matrices, and so the Jost matrices, and via them the S-matrix, become available on all sheets of the Riemann surfaces.

The proposed method for extracting resonance parameters from experimental cross-sections, thus relies on the proper analytic structure of the parametrized S-matrix. Since it is mathematically correct, the S-matrix obtained from the parametrization of the scattering data even allows the calculation of cross sections for channels where no experimental data is available.

Also, the S-matrix is fitted for real energies, but this allows the nearby complex resonance values to accurately be determined by means of the correctly factorised

Jost-matrices. The resonance parameters are the real and imaginary parts of the complex zeros of the Jost matrix determinant, which corresponds with the poles of the S-matrix. The real part corresponds with the energy at which the resonance occurs, and the imaginary part is linked to the resonance width, related to the half-life of the resonance. The channel widths are also accurately determined from the Jost matrices.

Apart from being rigorous and simple, one of the greatest advantages in the proposed method is that it takes into account long-ranged interactions. This is a huge improvement on [6], where the biggest limitation was the fact that the method was only applicable to short-ranged potentials.

Of course, there are still limitations. The method is most assuredly non-relativistic in nature, which means modelling intermediate and high-energy scattering is out of the question, unless relativistic corrections are made. This can be done using relativistic kinematics, as suggested in [6], where the channel momenta, k_n, are replaced with their corresponding relativistic expressions. This approach is particularly effective in meson-nuclear physics.

To sum up, it has successfully been shown that the proposed method can accurately be used to extract resonance parameters from low-energy scattering data involving Coulomb interaction. The next step would be to implement the method in a real scattering problem. This would certainly be useful in nuclear physics, but the method will specifically be applied in the regime of molecular physics, where it has been shown that the resonance phenomenon also occurs.

Bibliography

[1] D. J. Griffiths, *Introductory Quantum Mechanics*. Pearson Prentice Hall, second ed., 2005.

[2] J. R. Taylor, *Scattering Theory, The Quantum Theory of Nonrelativistic Collisions*. John Wiley & Sons, New York, second ed., 1972.

[3] S. A. Rakityansky and N. Elander, "Analytic structure of the multichannel Jost matrix for potentials with Coulombic tails," *Journal of Mathematical Physics*, vol. 54, no. 12, p. 122112, 2013.

[4] S. A. Rakityansky and N. Elander, "Analytic structure and power series expansion of the Jost function for the two-dimensional problem," *Journal of Physics A: Mathematical and Theoretical*, vol. 45, p. 135209, Apr. 2012.

[5] S. A. Sofianos and S. A. Rakityansky, "Exact method for locating potential resonances and Regge trajectories," *Journal of Physics A: Mathematical and General*, vol. 30, p. 19, July 1996.

[6] S. A. Rakityansky and N. Elander, "A method for extracting the resonance parameters from experimental cross section," *arXiv:1210.5995v1*, p. 22, Oct. 2012.

[7] S. A. Rakityansky, S. A. Sofianos, and K. Amos, "A method of calculating the Jost function for analytic potentials," *Nuovo Cimento*, vol. 111, p. 20, May 1995.

[8] S. A. Rakityansky and S. A. Sofianos, "Jost Function for Coupled Partial Waves," *Journal of Physics A*, vol. 31, p. 32, Feb. 1998.

[9] S. A. Rakityansky and S. A. Sofianos, "Jost function for coupled channels," *Nuclear Theory*, Aug. 1998.

[10] K. F. Riley, M. P. Hobson, and S. J. Bence, *Mathematical Methods for physics and engineering*. Cambridge University Press, 1998.

[11] J. Cullerne, *Penguin Dictionary of Physics*. Penguin Books, fourth ed., 2009.

[12] R. Jost *Helv. Phys. Acta*, no. XX, pp. 256–266, 1947.

[13] G. N. Watson, *A Treatise on the Theory of Bessel Functions*. Cambridge University Press, 1966.

[14] A. R. Edmonds, *Angular momentum in quantum mechanics*. Princeton University Press, New Jersey, 1957.

[15] S. A. Rakityansky and N. Elander, "Multi-channel analog of the effective-range expansion," *Journal of Physics A: Mathematical and Theoretical*, vol. 44, p. 33, Oct. 2011.

[16] S. A. Rakityansky and N. Elander, "Analyzing the contribution of individual resonance poles of the S-matrix to the two-channel scattering," *International Journal of Quantum Chemistry*, vol. 109, p. 51, Oct. 2011.

[17] L. S. Rodberg and R. M. Thaler, *Introduction to the Quantum Theory of Scattering*. Academic Press, New York and London, 1967.

[18] G. Springer, *Introduction to Riemann Surfaces*. Addison-Wesley, 1957.

[19] J. E. G. Farina, *Quantum Theory of Scattering Processes*. Pergamon Press, 1973.

[20] E. Lambert, "Fonction de portée effective et déplacement en énergie des états liés en présence d'un potentiel coulombien modifié," *Helv. Phys. Acta*, no. 42, pp. 667–677, 1969.

[21] L. Moneta, F. James, M. Winkler, and A. Zsenei, "Description of minuit code; http://seal.web.cern.ch/seal/snapshot/work-packages/mathlibs/minuit/."